

1 **Running head:** Chromatin profiles of maize florigen genes

2

3 Corresponding Authors:

4 Vincenzo Rossi: tel: +39 035313132 ex106 – E-mail: Vincenzo.Rossi@entecra.it

5 Joseph Colasanti: tel: 519-824-4120 ex58052 – E-mail: jcolasan@uoguelph.ca

6

7

8 Research area most appropriate for the paper: Genes, Development and Evolution

9 **Florigen-encoding genes of day-neutral and photoperiod-sensitive**
10 **maize are regulated by different chromatin modifications at the floral**
11 **transition¹**

12

13 **Iride Mascheretti, Katie Turner, Roberta S. Brivio, Andrew Hand², Joseph Colasanti,^{*} and**
14 **Vincenzo Rossi^{*}**

15

16 Consiglio per la Ricerca in Agricoltura e l'Analisi dell'Economia Agraria, Unità di Ricerca per la
17 Maiscoltura, I-24126 Bergamo, Italy (I.M., R.S.B., V.R.); Department of Molecular and Cellular
18 Biology, University of Guelph, N1G 2W1 Guelph, Ontario, Canada (K.T., A.H., J.C.)

19

20 **SUMMARY**

21 Florigen-encoding genes have different chromatin signatures associated with the floral transition in
22 photoperiod-responsive maize ancestor and modern temperate maize

23

24 ¹ This work was principally supported by special grants from Italian Ministry of Education,
25 University and Research (MIUR) and the National Research Council of Italy (CNR) for the
26 Epigenomics Flagship Project (EPIGEN). Additional funds were from European Commission
27 (AENEAS FP7 project KBBE-2009-226477). I.M. had a PhD fellowship funded by the Research
28 Agricultural Council (CRA) and in agreement with the University of Padova, Italy. Research in
29 V.R. lab was supported by Institutional grants from Italian Ministry of Agriculture, Food and
30 Forestry Policies (MiPAAF). Research in J.C. lab was supported by a Natural Sciences and
31 Engineering Research Council (NSERC) of Canada Discovery grant.

32

33 ² Present address: MedReleaf, L3R 6G4 Markham, Ontario, Canada.

34

35 * Address correspondence to Vincenzo.Rossi@entecra.it and jcolasan@uoguelph.ca.

36 The authors responsible for the distribution of materials integral to the findings presented in this
37 article in accordance with the polish described in the Instructions for Authors
38 (<http://www.plantphysiol.org>) are: Vincenzo Rossi (Vincenzo.Rossi@entecra.it) and Joseph
39 Colasanti (jcolasan@uoguelph.ca).

40

41 **ABSTRACT**

42 Activity of the maize florigen gene *Zea CENTRORADIALIS 8* (*ZCN8*) is associated with the floral
43 transition in both day-neutral temperate maize (*Zea mays*) and short-day (SD) requiring tropical
44 maize. We analyzed transcription and chromatin modifications at the *ZCN8* locus and its nearly
45 identical paralog *ZCN7*, during floral transition. This analysis was performed with day-neutral
46 maize (*Zea mays* ssp *mays*), where flowering is promoted almost exclusively via the autonomous
47 pathway through the activity of the regulatory gene *indeterminate 1* (*id1*), and tropical teosinte (*Zea*
48 *mays* ssp *parviglumis*) under floral-inductive and non-inductive photoperiods. Comparison of
49 *ZCN7/ZCN8* histone modification profiles in immature leaves of non-flowering *id1* mutants and
50 teosinte grown under floral inhibitory photoperiods reveals that both *id1* floral inductive activity
51 and SD-mediated induction result in histone modification patterns that are compatible with the
52 formation of transcriptionally competent chromatin environments. Specific histone modifications
53 are maintained during leaf development and may represent a chromatin signature that favors the
54 production of processed *ZCN7/ZCN8* mRNA in florigen-producing mature leaf. However, whereas
55 *id1* function promotes histone H3 hyper-acetylation, SD induction is associated with increased
56 histone H3 di- and tri-methylation at lysine 4. In addition, *id1* and SD differently affect the
57 production of *ZCN7/ZCN8* antisense transcript. These observations suggest that distinct
58 mechanisms distinguish florigen regulation in response to autonomous and photoperiod pathways.
59 Finally, the identical expression and histone modification profiles of *ZCN7* and *ZCN8* in response to
60 floral induction suggest that *ZCN7* may represent a second maize florigen.

61

62 INTRODUCTION

63

64 The transition from vegetative to reproductive development is triggered by a leaf-derived,
65 mobile floral-promoting signal named florigen (Chailakhyan, 1937; Giakountis and Coupland,
66 2008). In Arabidopsis (*Arabidopsis thaliana*), the protein encoded by the *FLOWERING LOCUS T*
67 (*FT*) gene has florigen activity (Corbesier et al., 2007; Jaeger and Wigge, 2007). All Arabidopsis
68 floral regulatory pathways, including the autonomous, gibberellin, photoperiod, and vernalization
69 pathways, converge on the *FT* gene, indicating that *FT* is a key integrator of floral inductive signals
70 (Turck et al., 2008). In the photoperiod pathway, *FT* transcription in the vasculature of mature
71 leaves is regulated by the direct binding of a protein encoded by *CONSTANS* (*CO*) in response to
72 long day (LD) growing conditions (Samach et al., 2000; Tiwari et al., 2010). *FT*, a
73 phosphatidylethanolamine-binding protein (PEBP), then moves from leaves through the phloem to
74 the shoot apical meristem (Corbesier et al., 2007; Jaeger and Wigge, 2007) where it interacts with a
75 bZIP transcription factor encoded by the *FLOWERING LOCUS D* (*FD*) locus to induce expression
76 of floral identity genes, such as *APETALA1* (Abe et al., 2005; Wigge et al., 2005). Recently, it was
77 shown that chromatin-related mechanisms play an important role in regulating *FT* expression (He et
78 al., 2012; Gu et al., 2013; Bu et al., 2014; Lopez-Gonzales et al., 2014; Wang et al., 2014).

79 *FT* orthologs have been discovered in diverse plant species, and many of these *FT*-related
80 genes are regulated differently depending on the photoperiod sensitivity or other floral inductive
81 requirements of the species (Andres and Coupland, 2012). In maize (*Zea mays*), a large PEBP gene
82 family named *Zea CENTRORADIALIS* (*ZCN*) was identified and found to include putative *FT*
83 orthologs (Danilevskaya et al., 2008). One of these genes, *ZCN8*, was shown to have the requisite
84 characteristics for florigenic activity (Lazakis et al., 2011; Meng et al., 2011). Indeed, *ZCN8* has
85 high sequence similarity to *FT*, exhibits a leaf-exclusive expression pattern, and *ZCN8* protein
86 interacts with DLF, the cognate maize ortholog of Arabidopsis FD protein (Muszynski et al. 2006;
87 Danilevskaya et al., 2008). Moreover, phloem-specific *ZCN8* expression in Arabidopsis rescues the
88 *ft* mutation (Lazakis et al., 2011) and, in maize, ectopic *ZCN8* expression causes earlier flowering in
89 transgenic plants, while silencing by artificial microRNA results in delayed flowering (Meng et al.,
90 2011). Quantitative trait locus (QTL) studies show that *ZCN8* is closely associated with *Vgt2*, a
91 major effect QTL for flowering time variation (Bouchet et al., 2013). Finally, *ZCN8* is up-regulated
92 upon the floral transition in day-neutral temperate maize and photoperiod-sensitive tropical maize
93 (Lazakis et al., 2011; Meng et al., 2011). Floral transition in maize temperate lines (e.g. the inbred
94 B73) occurs almost exclusively in response to endogenous signals by means of the autonomous

95 pathway and *ZCN8* expression in mature leaf is activated by the *indeterminate1* (*id1*) gene, which
96 encodes a monocot-specific zinc finger transcriptional regulator (Colasanti et al., 1998; Colasanti
97 and Coneva 2009; Lazakis et al., 2011). Conversely, in tropical maize, including the progenitor of
98 temperate maize, teosinte (*Zea mays* ssp *parviglumis*), which has an obligate requirement for short
99 day (SD) photoperiods to induce flowering, *ZCN8* is highly up-regulated in leaves under inductive
100 photoperiods (Lazakis et al., 2011; Meng et al., 2011). Therefore, these extreme maize varieties
101 present a unique opportunity to investigate the differences in florigen regulation between the
102 autonomous and photoperiod pathways.

103 The nature of the upstream mechanisms that control *ZCN8* expression in the leaf remains an
104 open question. A potential maize ortholog of Arabidopsis *CO*, *CONZ1*, was identified (Miller et al.,
105 2008), yet there is no indication that *CONZ1* directly activates *ZCN8* expression or that it regulates
106 maize flowering. In addition, although *id1* activates *ZCN8*, the temporal and spatial expression
107 patterns of the *id1* and *ZCN8* genes do not overlap because *id1* gene activity is confined to
108 immature developing leaves (Colasanti et al., 1998; Wong and Colasanti, 2007), whereas *ZCN8*
109 expression is detected only in mature leaves (Danilevskaya et al., 2008). Therefore it is unlikely that
110 *ZCN8* is a direct target of the ID1 protein. One possibility is that ID1 protein operates by means of
111 epigenetic mechanisms to promote the formation of a transcriptionally competent *ZCN8* chromatin
112 in immature leaf, which is maintained throughout leaf development to enable production of
113 florigenic signals in the mature leaf. The relevance of epigenetic mechanisms in maize flowering
114 was demonstrated recently with the finding that the *nucleosome remodeling factor complex*
115 *component101* (*nfc101*) and *nfc102* genes encode WD-repeat proteins that bind both *id1* and *ZCN8*
116 sequences, thus regulating their expression and chromatin modifications (Mascheretti et al., 2013).

117 In the present study, we provide evidence that chromatin modifications are involved in *id1*-
118 mediated regulation of *ZCN8* expression in temperate, day-neutral maize. Unexpectedly a different
119 histone modification pattern of *ZCN8* chromatin during leaf development was detected in response
120 to SD-dependent floral induction in teosinte. These findings highlight both conserved and divergent
121 features of florigen regulation between autonomous and photoperiod-regulated pathways.
122 Furthermore, analysis of *ZCN7*, a highly similar paralog of *ZCN8* (Danilevskaya et al., 2008),
123 shows that both genes have identical expression and chromatin profiles, suggesting that *ZCN7* may
124 encode another maize florigen.

125

126 RESULTS

127

128 **Identification and isolation of *ZCN7* and *ZCN8* gene sequences**

129

130 Previous phylogenetic analysis of *ZCN* genes suggests that *ZCN7* and *ZCN8* represent
131 paralogs arising from the tetraploid ancestry of maize (Danilevskaya et al., 2008). *ZCN7* and *ZCN8*
132 genomic and cDNA sequences are publically available. However, the *ZCN8* sequence was
133 identified in the maize B73 inbred line (GenBank accession number EU241899), while the *ZCN7*
134 sequence was identified in the Gaspé Flint early flowering line. In addition, the *ZCN8* cDNA
135 corresponding to the processed mRNA was isolated from mature leaf of B73 inbred, whereas only
136 the unspliced version of the *ZCN7* cDNA was obtained in the Gaspé Flint line (Danilevskaya et al.,
137 2008). In the present study we identified *ZCN7* genomic and cDNA sequences from the B73 inbred
138 (GenBank accession number KP202720) and isolated a sequence representing the processed mRNA
139 for the *ZCN7* gene from mature leaf of this line (Supplemental Fig. S1; see below for details
140 regarding specific *ZCN7* and *ZCN8* transcripts analysis).

141 For the purposes of analyzing expression in teosinte, we sequenced the teosinte *ZCN7* and
142 *ZCN8* genes and cDNAs. The *ZCN7* and *ZCN8* genomic sequences were identified using a PCR-
143 based method (see Supplemental Materials and Methods) and their respective coding sequences
144 were subsequently identified by synthesizing cDNA from total RNA of teosinte mature leaf
145 followed by RT-PCR with primers located close to the start and stop codons. Even though teosinte
146 is considered a wild relative of maize, we detected no sequence heterogeneity in the *ZCN* genes
147 isolated from teosinte. Sequence similarity between B73 *ZCN7* and *ZCN8* genes and their orthologs
148 in teosinte are reported in Supplemental Table S1.

149

150 **Experimental conditions for analyzing *ZCN7* and *ZCN8* regulation during leaf development
151 and in response to floral induction**

152

153 The major aim of this study is to analyze *ZCN7* and *ZCN8* regulation when the plant is
154 committed to flower and in early and later stages of leaf development. This provides a framework
155 for determining whether and how chromatin modification patterns might be established at florigen
156 genes in response to floral inductive cues and maintained during leaf development. To this end,
157 immature and mature leaf samples were obtained from *id1* mutant segregating plants introgressed
158 into the B73 background at the V6/V7 developmental stage (i.e., seedlings with the 6th or 7th leaf
159 fully extended with collars and the 8th/9th leaves visible; Fig. 1). This stage corresponds to the
160 vegetative to reproductive phase transition in B73 inbred (Coneva et al., 2007; Lazakis et al., 2011).

161 Moreover, the immature leaf tissue used for analysis (Supplemental Fig. S3) represents where the
162 *id1* gene is expressed, while the *ZCN8* processed mRNA is not yet produced (Colasanti et al., 1998;
163 Wong and Colasanti, 2007; Meng et al., 2011). In contrast, mature leaf expresses *ZCN8* mRNA, but
164 *id1* transcript and ID1 protein are not detected. To characterize more precisely *ZCN7* and *ZCN8*
165 mRNA localization during leaf development, we carried out quantitative RT-PCR (qRT-PCR) with
166 primers conserved in the two paralogs and using RNA obtained following leaf blade dissection of
167 pre-transition (V4), transition (V6) and post-transition (V8) stage plants (Supplemental Fig. S2).
168 This analysis showed that *ZCN7/ZCN8* mRNA is most abundant in the distal portions of adult leaf
169 blades and much less so in juvenile leaves at all three stages of development. *ZCN7/ZCN8*
170 expression was not detected in blade sheaths or in non-photosynthetic regions of immature leaves.
171 Interestingly, transcript levels continued to increase well after the floral transition (V8 leaves),
172 suggesting a possible role for *ZCN7/ZCN8* in reproductive development. On the basis of these
173 observations we decided to employ the leaf blades of V6/V7 transition stage plants for the analysis
174 of *ZCN7/ZCN8* transcripts and chromatin modifications (Supplemental Fig. S3). A parallel analysis
175 of the same tissues was performed with teosinte plants harvested at the analogous developmental
176 stage. In this case, the floral transition was induced by growing plants under SD conditions, while
177 flowering was inhibited in a parallel set of plants by interrupting the long night with one hour of
178 light. We previously showed that this night break (NB) regimen effectively prevents flowering in
179 teosinte without greatly altering the total amount of light received by non-flowering plants relative
180 to those grown under SD conditions (Fig. 1; Lazakis et al., 2011; Coneva et al., 2012).

181

182 Analysis of specific *ZCN7* and *ZCN8* transcripts

183

184 A previous analysis of *ZCN7* and *ZCN8* transcription using locus-specific primers located
185 near start and stop codons revealed that the *ZCN8* locus gives rise to a mixture of spliced and
186 unspliced *ZCN8* transcripts in leaf blade of the maize B73 inbred, while only an unspliced form was
187 detected in immature leaf and other maize tissues (Danilevskaya et al., 2008). Conversely, only
188 unspliced *ZCN7* transcript was detected in all maize tissues analyzed in the maize Gaspé Flint line.
189 Using primer combinations to the same regions we confirmed these results in B73 immature and
190 mature leaf samples (Fig. 2A). However, when we used a *ZCN7* specific forward primer located 75
191 bp downstream of that employed by Danilevskaya et al. (2008; Fig. 2A, primer ZCN7-1b instead of
192 ZCN7-1a) the *ZCN7* gene showed the same pattern of transcript accumulation reported for *ZCN8*,
193 including the production of spliced mRNA in mature leaf (Fig. 2A). Similar results were obtained in

194 mature and immature leaves of teosinte plants grown under floral inductive SD conditions. This
195 indicates that, in mature leaf of the B73 inbred and in teosinte, *ZCN7* produces a processed mRNA
196 that encodes a putative polypeptide. It is worth mentioning that the expression pattern we observe
197 for *ZCN7* and *ZCN8* is supported by data from RNA-seq studies (Supplemental Table S2; Sekhon et
198 al., 2013), which can distinguish among highly similar *ZCN* paralogs, thus indicating that both
199 *ZCN7* and *ZCN8* are detected predominantly in mature leaf blade.

200 A recent report used a combination of RNA blotting with strand specific probes and RT-
201 PCR with locus and strand-specific primers to show that *ZCN8* produces three transcript isoforms
202 (Mascheretti et al., 2013). These isoforms correspond to: i) the processed sense mRNA, which
203 accumulates only in mature leaf; ii) a very low amount of unspliced sense strand pre-mRNA present
204 both in meristematic enriched regions and in mature leaf; and iii) an unspliced antisense RNA
205 strand, which represents the prevalent form of unspliced transcript and is produced not only in
206 leaves, but also in various other tissues (Figure 2C). This observation indicates that, to study *ZCN8*
207 transcription in detail, it is necessary to employ a method that can distinguish all three RNA
208 isoforms. Accordingly, we performed strand-specific RT-PCR to differentiate the *ZCN7* and *ZCN8*
209 transcript isoforms present in leaves of wild-type B73 and SD-induced teosinte plants. Our results
210 reveal that *ZCN7* and *ZCN8* produce the same three transcript isoforms in the B73 inbred and that
211 these isoforms are present also in teosinte plants (Fig. 2B and Fig. 2C). We cloned and sequenced
212 cDNAs derived from the *ZCN7* and *ZCN8* antisense RNAs of B73 and teosinte plants and found
213 that they encode very short putative ORFs with no homology with known proteins (Supplemental
214 Fig. S4; Mascheretti et al., 2013). Therefore these antisense transcripts may represent long non-
215 coding RNAs (lncRNAs). Collectively our results indicate that the highly similar *ZCN7* and *ZCN8*
216 transcripts also exhibit an analogous expression profile in B73 and teosinte.

217

218 **Variation of *ZCN7* and *ZCN8* transcript isoform levels under floral-inductive vs non-inductive
219 conditions**

220

221 Strand-specific qRT-PCR was employed to analyze the abundance of *ZCN7* and *ZCN8*
222 transcript isoforms under conditions that reduce florigen production; namely, absence of *id1*
223 function in temperate maize and non-inductive NB conditions in tropical teosinte plants. We found
224 that processed sense mRNA levels of *ZCN7* and *ZCN8* decrease in mature leaves of the *id1* mutant
225 compared to wild-type mature leaves and that this occurs with a concomitant reduction of unspliced
226 sense pre-mRNA and an increase of unspliced antisense strand in the same tissues (Fig. 3A). The

same pattern was observed in B73 immature leaf, except that in these samples spliced sense mRNA was not detected. In contrast, a different pattern of isoform transcript variation was observed in teosinte plants. Mature leaves from plants grown under non-inductive NB conditions have less *ZCN7* and *ZCN8* processed and unspliced sense oriented mRNA levels compared to plants grown under inductive SD conditions; however, antisense strand levels were unaffected (Fig. 3B). No variation in antisense RNA accumulation was observed and a decrease in unspliced pre-mRNA levels was also detected in teosinte immature leaf. It is worth noting that the magnitude of the decrease of *ZCN7* and *ZCN8* sense transcript levels is much higher in mature leaf of teosinte under non-inductive NB conditions than in mature leaf of the *id1* late flowering mutant (Fig. 3A and Fig. 3B). This effect may be correlated with the higher *ZCN7* and *ZCN8* transcript levels detected in mature leaves of teosinte under floral inductive SD conditions compared to wild-type B73 (Supplemental Fig. S5; Lazakis et al. 2011). Although higher levels of *ZCN7* and *ZCN8* RNA are more pronounced for the sense pre- and processed-mRNA, it is also evident for the antisense strand. Conversely, no differences in transcript isoform abundance were detected in immature leaves of B73 and teosinte.

Overall these results indicate that both *ZCN7* and *ZCN8* mRNAs are positively regulated by factors that induce flowering (i.e. *id1* gene function in autonomously flowering maize and SD photoperiod-requiring teosinte). However, only functional *id1* concomitantly affects the abundance of antisense orientated RNA strand of these genes, suggesting that regulation of *ZCN7/ZCN8* putative antisense lncRNAs is limited to the *id1*-regulated flowering pathway and not the photoperiod pathway.

248

249 **Correlation of histone modifications in B73 *ZCN7* and *ZCN8* chromatin with *id1* gene activity**

250

251 Histone modifications are marks of chromatin transcriptional status (Lauria and Rossi, 2011). Therefore we analyzed the histone profiles of the *ZCN7* and *ZCN8* genes in temperate maize 252 to understand whether and how histone modifications are correlated with the *id1*-mediated 253 activation of these genes. Chromatin immunoprecipitation (ChIP) assays were performed to analyze 254 histone modifications in different regions of the *ZCN7* and *ZCN8* genes (Fig. 4 and Supplemental 255 Fig. S6). We selected histone marks that are usually located within genes and that were previously 256 analyzed for florigen genes of other plant species (Jiang et al., 2008; Adrian et al., 2010; He et al., 257 2012; Sun et al., 2012; Gu et al., 2013; Mascheretti et al., 2013; Lopez-Gonzales et al., 2014). Four 258 histone marks usually associated with active transcription were selected for chromatin analysis. 259

260 These are: histone H3 acetylated at lysine 9 and 14 (H3ac), histone H3 di- and tri-methylated at
261 lysine 4 (H3K4me2 and H3K4me3), and histone H3 di-methylated at lysine 36 (H3K36me2). In
262 addition, we examined histone H3 tri-methylation at lysine 27 (H3K27me3) as a representative
263 repressive euchromatin mark. Finally, an antibody against the histone H3 C-terminal region
264 (H3Cter) that recognizes histone H3 independently of any post-transcriptional modifications was
265 used as an estimate of nucleosome density, which is a useful metric for normalizing data generated
266 in histone modification analyses (Rossi et al., 2007).

267 We observed that the pattern of histone modifications at *ZCN7* and *ZCN8* chromatin was
268 very similar and that the histone marks analyzed can be divided into four groups based on their
269 correlation with the activity of the *id1* gene. These results are illustrated in Figure 4 and
270 Supplemental Figure S6 and are summarized schematically in Figure 6. The first group includes
271 H3ac, which exhibits significantly higher levels in both immature and mature leaves of wild-type
272 plants relative to *id1* mutant leaves in all genomic regions analyzed. Conversely, in the second
273 group the repressive H3K27me3 mark was detected at higher levels in immature leaves of *id1*
274 mutant relative to wild-type, while in mature leaves H3K27me3 was prevalent at the 5'-end regions
275 of *ZCN7* and *ZCN8* independently of normal *id1* function. The active marks H3K4me3 and
276 H3K36me2, similar to H3ac, were higher in mature leaves of wild-type plants relative to *id1* mutant
277 mature leaves. However, unlike H3ac, these marks were present at similar levels in immature leaves
278 of both wild-type and *id1* mutant plants, thus defining a third group. Finally, the fourth group
279 includes H3K4me2 and the nucleosome occupancy, which were independent of *id1* gene activity for
280 both immature and mature leaf. Since nucleosome occupancy is not affected by *id1*, the statistical
281 significance of the observed changes in histone modifications was not influenced by the correction
282 for nucleosome density (Fig. 4 and Supplemental Fig. S6).

283 This analysis also provides information about the features of chromatin modification at
284 florigen genes in temperate maize. First, the changes detected are consistent for all analyzed
285 genomic regions of *ZCN7* and *ZCN8*. Second, the *ZCN7* and *ZCN8* loci in both immature and
286 mature leaves of florally-competent wild-type plants are characterized by the presence of histone
287 marks associated with active chromatin, suggesting that an open chromatin structure is present
288 through all stages of leaf development. Third, localization of some histone marks within the *ZCN7*
289 and *ZCN8* loci was different than expected. That is, H3K4me3 was enriched in the 3'-end, while it
290 usually exhibits a peak in the 5'-end region and H3K27me3 accumulated in the 5'-end region, while
291 it usually is located in the gene body (Lauria and Rossi, 2011).

292

293 **Correlation of histone modifications in teosinte *ZCN7* and *ZCN8* chromatin with SD-induced
294 flowering**

295

296 The same ChIP assays used to analyze histone modifications in B73 plants were carried out
297 with SD (induced) and NB (uninduced) teosinte plants (Fig. 5, Supplemental Fig. S7 and Fig. 6).
298 As described above for B73 with respect to *id1* gene activity, the histone modification variation
299 between SD and NB conditions allows the subdivision of the histone marks into different groups
300 based on changes in response to SD floral induction. The first group includes H3K4me2 and
301 H3K4me3, which were enriched in *ZCN7* and *ZCN8* in immature leaves of SD grown plants and are
302 maintained at high levels in mature leaf. The second group is typified by H3K36me2, which
303 increased in response to SD only in mature leaf. The third group includes H3ac, H3K27me3 and the
304 nucleosome density assay, which displayed no variation between SD and NB conditions. It is worth
305 noting that histone marks altered in response to SD floral induction in teosinte are different
306 compared to those affected by *id1* in the B73 inbred (Fig. 6). In addition, H3K27me3 was not
307 detected in *ZCN7* and *ZCN8* chromatin of teosinte plants. Although a direct comparison between
308 photoperiodic and autonomous flowering may require consideration of the different growth
309 conditions, these observations suggest that distinct chromatin modification mechanisms occur for
310 regulating florigen expression in response to the autonomous and photoperiod pathways.
311 Nevertheless, our analysis also reveals that some of the chromatin modifications features reported
312 for temperate maize are similarly found in teosinte. These include a similar histone modification
313 pattern correlated with SD floral induction exhibited by the *ZCN7* and *ZCN8* teosinte paralogs, the
314 absence of nucleosome occupancy variation between SD and NB conditions, the presence of histone
315 marks linked to active chromatin already detectable in immature leaf, and the unexpected
316 distribution pattern of H3K4me3.

317

318 **DNA methylation at *ZCN7* and *ZCN8* in B73 and teosinte plants**

319

320 DNA methylation is another epigenetic mark that can affect gene transcription (Lauria and
321 Rossi, 2011). Therefore we analyzed whether DNA methylation variation at the *ZCN7* and *ZCN8*
322 loci is associated with *id1* gene activity in temperate maize or SD induction in tropical teosinte.
323 First, we estimated the global cytosine methylation (mC) level in the same genomic regions
324 previously analyzed by ChIP assays. This was done with the methylation-dependent restriction
325 enzyme MspJI, which cleaves methylated DNA and can detect mC in all sequence contexts (CG,

326 CHG, CHH; where H = A, C, or T; Cohen-Karni et al., 2011). Results indicate that all regions
327 analyzed are methylated, but mC levels in both immature and mature leaf were not different in *id1*
328 mutant tissue compared to wild-type B73, nor did it vary in teosinte grown under SD and NB
329 conditions (Supplemental Fig. S8). To further validate these results and to examine possible mC
330 variation in a specific sequence context, three *ZCN7* and *ZCN8* genomic regions, representing the
331 5'-end, gene body, and 3'-end of the genes, were selected for bisulfite sequencing analysis with
332 genomic DNA extracted from B73 and teosinte immature leaves. We focused on this tissue to
333 assess whether mC variation is already established at *ZCN7* and *ZCN8* loci in immature leaf and in
334 response to floral inductive conditions. We also carried out bisulfite sequencing analysis of the 5'-
335 end putative *cis*-regulatory region of *ZCN8* in mature leaf. We detected no statistically significant
336 variation of mC in any of the sequence contexts in the comparison of B73 wild-type with *id1*
337 mutant or in teosinte SD with NB plants (Supplemental Fig. S9, Fig. S10, Fig. S11, Fig. S12, and
338 Supplemental Table S3). These results suggest that cytosine methylation is not a factor in *ZCN7* and
339 *ZCN8* regulation with respect to floral induction as mediated by *id1* function in temperate maize or
340 by SD photoperiod in tropical teosinte. Nonetheless, our analysis indicates that *ZCN7* and *ZCN8*
341 genes are methylated and that methylation occurs almost exclusively in the CG sequence context.
342

343 DISCUSSION

344

345 **Specific histone modification patterns in *ZCN7* and *ZCN8* chromatin are associated with**
346 **competence to flower in response to *id1* gene activity in temperate maize**

347

348 In the development of modern temperate maize from its tropical progenitor, teosinte, ancient
349 farmers selected variants with a flowering habit that is less influenced by photoperiod. The *id1* gene
350 is a key regulator of flowering in temperate maize, with loss of *id1* function causing a severe delay
351 in the floral transition (Colasanti and Muszynski, 2009). Thus comparison of *id1* mutants with
352 normal flowering plants provides an opportunity to study elements of the autonomous flowering
353 pathway in maize. The present study finds that *id1*-mediated regulation of *ZCN7* and *ZCN8*
354 expression in temperate maize is associated, at least in part, with chromatin-related mechanisms
355 (Fig. 7). An interesting observation from our study is that, in immature leaves of wild-type maize
356 plants at the floral transition, despite not producing florigen, the *ZCN7/ZCN8* loci are characterized
357 by a histone modification pattern (i.e. the presence of H3ac, H3K4me2, H3K4me3, and
358 H3K36me2) that is usually linked to active chromatin. In addition, the high CG methylation level

359 that we detect at *ZCN7* and *ZCN8* is compatible with a transcriptionally competent or active status,
360 as supported by an mC genome-wide distribution study in maize (Regulski et al., 2013). In
361 agreement with these observations, low-level accumulation of *ZCN7* and *ZCN8* sense pre-mRNA
362 and a higher level of the antisense RNA are detected in immature leaf. ChIP assays of *id1* mutant
363 immature leaves indicate that the majority of histone marks analyzed is not related to *id1* function,
364 suggesting that, additional factors must be involved. For example, some of these factors could be
365 chromatin remodeling complexes containing WD-repeat proteins NFC101/NFC102, which directly
366 bind *ZCN8* to negatively regulate its expression and H3K4me2 levels in meristem-enriched tissues
367 (Mascheretti et al., 2013). Nevertheless, we report that *id1* function is required to specify high H3ac
368 levels and to prevent H3K27me3 accumulation at *ZCN7/ZCN8* chromatin in immature leaf. More
369 importantly, *id1* activity is essential to maintain histone H3 hyper-acetylation in mature leaf, where
370 the *id1* gene is not expressed. This supports the involvement of epigenetic mechanisms, mediated
371 by *id1* activity, which facilitate production of *ZCN7/ZCN8* processed mRNAs in mature leaf, even
372 though *id1* mRNA and ID1 protein accumulation do not coincide with *ZCN7/ZCN8* expression.
373 Thus, in the proposed model (Fig. 7) *id1* induces histone H3 hyper-acetylation at florigen genes to
374 establish a transcriptionally competent chromatin environment in early stages of leaf development.
375 A previous study showed that chromatin modifications that are established at the *Arabidopsis*
376 *FLOWERING LOCUS C (FLC)* in actively dividing cells of developing tissues are maintained in
377 later stages of development (Finnegan and Dennis, 2007). Accordingly, our findings suggest that
378 also the chromatin status established at *ZCN7/ZCN8* in developing maize leaves by the *id1*-
379 mediated autonomous pathway is maintained throughout leaf development, until the formation of
380 mature leaves, where it may facilitate the synthesis of *ZCN7/ZCN8* processed mRNAs by means of
381 still unknown factors. In this scenario, *id1* acts as a “gatekeeper” that primes floral induction in day-
382 neutral temperate maize. Previous transcriptome comparisons of flowering and non-flowering
383 maize suggest that *id1* also regulates genes involved in primary metabolism to establish a
384 physiological state associated with readiness for flowering (Coneva et al., 2007; Coneva et al.,
385 2012), thus connecting florigen production with metabolic rate to facilitate the transition to
386 reproductive growth.

387 Our study shows that *id1* function is correlated with increased H3K4me3 and H3K36me2
388 levels at *ZCN7/ZCN8* chromatin only in mature leaf, although the *id1* gene is not expressed in these
389 tissues. This could be explained by an indirect effect related to *id1*-dependent activation of
390 *ZCN7/ZCN8* sense mRNA levels in mature leaf. Indeed, it is widely documented that, in many
391 cases, transcription drives accumulation of histone marks associated with active chromatin and not

392 vice versa (Henikoff and Shilatifard, 2011). In addition, our analysis provides no evidence as to
393 whether ID1 protein directly or indirectly regulates histone modifications at *ZCN7* and *ZCN8*.
394 However, *ZCN7* and *ZCN8* sequences have no apparent ID1 protein binding sites (Kozaki et al.,
395 2004). Moreover, the putative rice (*Oryza sativa*) *id1* ortholog (*RID1*, *OsId1*, or *Ehd2*) activates
396 *Hd3a* florigen by promoting the expression of transcription factor *Ehd1* (Matsubara et al., 2008;
397 Park et al., 2008; Wu et al., 2008). Therefore, it is possible that ID1 protein does not interact
398 directly with florigen gene regulatory elements.

399

400 **Photoperiod floral inductive pathway alters *ZCN7* and *ZCN8* chromatin modifications in
401 tropical teosinte differently than the autonomous pathway in B73 temperate maize**

402

403 Teosinte was selected for this analysis because it represents maize with an obligate
404 requirement for SD photoperiods to induce flowering. Although it is difficult to make direct
405 comparisons of photoperiod-induced versus autonomously regulated flowering because the plants
406 were exposed to different growth conditions, examination of chromatin modifications of florigen
407 genes could reveal some commonalities and differences. Whereas autonomous flowering is
408 controlled by endogenous signals, photoperiod-induced flowering represents an immediate response
409 to inductive signals. Therefore comparison of the chromatin profiles associated with these different
410 pathways could reveal underlying mechanisms implicit to these different floral induction strategies.
411 Similar to *id1*-controlled flowering via the autonomous pathway in temperate maize, we found that
412 SD-induced florigen activation in teosinte promotes the formation of a particular histone
413 modification pattern at *ZCN7/ZCN8* loci during leaf development (Fig. 7). However, unlike *id1*
414 regulation in B73, SD floral induction in teosinte promotes increased H3K4me2 and H3K4me3
415 levels in both immature and mature leaves, but does not affect histone H3 acetylation. This suggests
416 that distinct mechanisms, perhaps reflecting the different ways that various histone modifications
417 influence transcription (Bannister and Kouzarides, 2011), distinguish the *id1*- and SD-related
418 regulation of *ZCN7/ZCN8* expression. Another difference between the two florigen-regulatory
419 pathways is that the H3K27me3 repressive mark is present at the 5'-end of *ZCN7/ZCN8* chromatin
420 only in mature leaf of wild-type maize, but is not detected in teosinte. This difference could have
421 functional implications given that a genome-wide analysis found limited H3K27me3 variation in
422 the same tissues of different maize inbreds (Makarevitch et al., 2013). In particular, the presence of
423 H3K27me3 may be associated with overall lower levels of the *ZCN7* and *ZCN8* transcript isoforms
424 detected in mature maize leaf compared to mature leaf of teosinte. Indeed, H3K27me3 in the 5'-

regions attenuates the transcription of expressed mammalian genes (Young et al., 2011). This could also explain the unusual localization of H3K27me3 in the 5'-end region of florigen chromatin only (Luria and Rossi, 2011). Alternatively, the unexpected localizations of H3K27me3 and H3K4me3 in the 5'- and 3'-end regions, respectively, could be associated with transcription of *ZCN7/ZCN8* antisense RNA. Indications from extensively characterized eukaryotic transcriptional regulatory models suggest that *ZCN7/ZCN8* antisense lncRNAs may be involved in florigen regulation through various mechanisms, including chromatin modification (De Lucia and Dean, 2011). Although precise characterization of *ZCN7* and *ZCN8* antisense transcripts is beyond the scope of this study, we provide evidence that their regulation is different with respect to autonomous and photoperiod flowering pathways. Specifically, the antisense RNA level is inversely correlated with *id1* gene activity in B73 maize, yet unaffected by photoperiod in teosinte. The significance of this difference is an intriguing feature in future studies to investigate the function of *ZCN7/ZCN8* antisense RNAs.

437

438 ***ZCN7* may be a second maize florigen gene**

439

440 We found that the specific accumulation pattern of a spliced sense mRNA in mature leaf
441 previously detected for *ZCN8* (Danilevskaya et al., 2008) occurs also for its paralog *ZCN7*. The
442 discrepancy between our findings and those reported by Danilevskaya et al. (2008) may be due to
443 genotype-related differences of *ZCN7* in producing transcript splicing variants, since this early
444 study analyzed *ZCN7* expression in the Gaspé Flint line, while our study analyzed inbred B73 and
445 teosinte. Alternatively, the forward primer used to amplify *ZCN7* cDNA in the previous study may
446 not be within the *ZCN7* processed sense mRNA, because using this primer we were also unable to
447 detect the spliced variant in B73 and teosinte. In addition to the ability of both paralogs to produce
448 the processed mRNA, our results provide evidence that *ZCN7* and *ZCN8* exhibit a pattern of
449 transcript isoform accumulation and histone modifications that are affected identically by the *id1*
450 gene in wild-type maize and SD photoperiod in teosinte. Collectively, these findings support a
451 functional analogy between *ZCN7* and *ZCN8*, implying that *ZCN7* may encode a second maize
452 florigen. Meng et al. (2011) reported that the *ZCN7* sequence identified in Gaspé Flint does not
453 exhibit some of the properties of a florigen. For example, they found that, unlike *ZCN8*, *ZCN7*
454 protein interacted only weakly with maize FD ortholog, DLF1. Further, ectopic expression of *ZCN7*
455 cDNA in transgenic maize did not cause the minor yet significant acceleration of flowering
456 displayed by *ZCN8*-expressing lines. Since the genomic *ZCN7* sequence was used for transgenic
457 plant production it is possible that the absence of the early flowering phenotype observed by Meng

458 et al. (2011) could be due to the above mentioned inability of the Gaspé Flint *ZCN7* sequence to
459 produce processed mRNA. Alternatively, the function of *ZCN7* and *ZCN8* paralogs may not be
460 fully redundant, with *ZCN8* having higher florigenic activity. Nevertheless, here we show that,
461 similar to *ZCN8*, *ZCN7* is responsive to both *id1*-regulated and SD-mediated floral induction, an
462 important florigen feature that was not tested for the *ZCN7* gene (Meng et al., 2011). In addition,
463 *ZCN7* lies within a flowering time QTL, as does *ZCN8* (Bouchet et al., 2013). Further extensive
464 studies would be required to definitively demonstrate whether *ZCN7* possesses florigenic activity
465 similar to *ZCN8*.

466

467 Unique features of maize florigen regulation compared to other plants

468

469 In this study we describe features of florigen regulation that appear to be unique to maize.
470 First, the production of florigen antisense transcripts in both temperate maize and teosinte has not
471 been reported for other species. Second, we identified *ZCN7* and *ZCN8* unspliced sense pre-mRNAs
472 that have not been detected for florigen genes in other species. These pre-mRNAs are particularly
473 abundant in teosinte mature leaf tissue and their presence suggests that post-transcriptional RNA
474 processing mechanisms may play a role in florigen regulation (Mascheretti et al., 2013). Third, the
475 patterns of histone modifications at *ZCN7/ZCN8* loci in maize and teosinte are somewhat different
476 from those described for florigen genes from other species. For example, the presence of
477 H3K27me3 in Arabidopsis *FT* chromatin is correlated with repression of this gene (Turck et al.,
478 2007; Adrian et al., 2010; Wang et al., 2014), whereas in B73 maize H3K27me3 at *ZCN7/ZCN8* is
479 detected only in mature leaf, which is the tissue with maximum florigen production. This suggests
480 that, unlike Arabidopsis, H3K27me3 deposition in maize mature leaf is not associated with the
481 formation of fully repressive chromatin. Nevertheless, it is worth noting that, in immature leaves of
482 *id1* mutant, H3K27me3 accumulates in all *ZCN7/ZCN8* genomic regions. Since *id1* is also involved
483 in the control of the *ZCN7/ZCN8* sense and antisense unspliced RNA isoforms production at this
484 developmental stage (i.e. *id1* activity is correlated with the increase of sense and decrease of
485 antisense RNA strands), these findings indicate a possible role for *id1* in modulating the rate of
486 sense/antisense production through chromatin modifications. Histone acetylation represents another
487 difference between maize and Arabidopsis florigen genes. Indeed, in Arabidopsis H3ac is correlated
488 with photoperiod regulation of *FT* (Adrian et al. 2010; Gu et al., 2013), but it is unaffected by
489 photoperiod in teosinte and altered in the *id1*-controlled autonomous pathway in maize.

490 Overall, we find that maize employs unique mechanisms to regulate florigen production. We
491 also show that distinct chromatin modification patterns characterize florigen genes in leaves of
492 autonomously regulated maize plants compared to teosinte plants that rely on photoperiod
493 induction. These findings reveal a key role for chromatin-related epigenetic mechanisms in
494 controlling environmental adaptations to maize flowering and are thus important for elucidating the
495 regulatory underpinnings of flowering.

496

497 MATERIALS AND METHODS

498

499 Plant materials and growth conditions

500

501 Maize (*Zea mays* spp. *mays*) seeds segregating the *id1-m1* mutant allele backcrossed ten
502 times into the B73 inbred background were planted in soil (50% Sunshine Mix, 50% Turface clay)
503 in Conviron growth chambers under conditions of broad-spectrum light at 1000 $\mu\text{M}/\text{m}^2/\text{s}$. The *id1-*
504 *m1* mutant allele and wild-type segregating plants (Colasanti et al., 1998) were identified by PCR
505 genotyping as described previously (Wong and Colasanti, 2007). All maize plants were grown
506 under LD conditions (14 hours light/10 hours dark) with day temperatures of 25 °C and night
507 temperatures of 21 °C. Conversely, teosinte (*Zea mays* spp. *parviglumis*) plants were grown initially
508 in a growth chamber under non-inductive NB conditions of 9 hours day/7hours night/1hour light/7
509 hours night for 27 days (approximately 8 visible leaves), after which one half of the plants were
510 transferred to a SD growth chamber at 10 hours day/14hours night. Prior to growing plants for this
511 experiment we determined that plants exposed to a 1 hour exposure to daylight conditions in the
512 middle of the long dark period (night break: NB) treatment were effectively inhibited in flowering
513 in 100% of teosinte plants, as determined by examining shoot apex structure at various time points
514 (Fig. 1 and K. Turner and J. Colasanti, unpublished).

515 Plants at the V6/V7 stage corresponding to the floral transition in maize B73 inbred, or 10
516 days after growth of teosinte plants under NB conditions (Fig. 1), were used for isolation of the
517 tissues employed in the analysis of *ZCN7/ZCN8* transcripts and in ChIP assays. Mature and
518 immature leaf tissues were sampled. Specifically, for maize B73 inbred plants, tissues of mature
519 leaves were obtained by isolating the distal 30 cm of blade tissue from leaf 8, while the immature
520 leaf tissue from the same plant consisted of the central cylinder of non-photosynthetic developing
521 leaves from 2 cm to 12 cm above the shoot apex, sampled as reported in Colasanti et al. (1998).
522 Details of the sampling strategy are illustrated in Supplemental Fig. S3. For induced and uninduced

523 teosinte plants, the mature leaf samples were obtained by harvesting the distal 30 cm of the
524 youngest mature leaf with an exposed collar, usually leaf 8 or 9. Immature leaves, 2 to 12 cm above
525 the shoot apex, were harvested as described for maize. For each biological replication a minimum
526 of five plants were harvested. For *ZCN7/ZCN8* mRNA expression analysis during the course of
527 maize development (Supplemental Fig. S2), leaves from B73 inbred were harvested from V4, V6
528 and V8 stage plants at the mid-point of the day light cycle. Whole leaf blade was used for small
529 leaves (< 10 cm) or leaves were dissected into halves, thirds or quarters for larger leaves, as shown
530 in Supplemental Fig. S2.

531

532 **cDNA synthesis and RT-PCR**

533

534 Total RNA extraction and oligo(dT)-primed and strand-specific cDNA synthesis were performed as
535 previously described (Mascheretti et al., 2013). Sequences of locus-specific primers used for strand-
536 specific reverse transcription are reported in Supplemental Table S4. Conditions for PCR
537 amplification of maize B73 and teosinte full length *ZCN7* and *ZCN8* cDNAs were as described by
538 Danilevskaya et al. (2008), with primers located close to the start and stop codons (Supplemental
539 Table S5). Conditions for strand-specific RT-PCR amplification and subsequent cloning of B73 and
540 teosinte *ZCN7/ZCN8* cDNAs produced by unspliced sense and antisense RNAs were as previously
541 reported (Mascheretti et al., 2013; see Supplemental Table S5 for the list of PCR primers). Real-
542 time qRT-PCR was performed and amount of changes between samples calculated using the $2^{-\Delta\Delta Ct}$
543 method as previously described by Rossi et al. (2007). cDNA preparations from two biological
544 replicates were made and three replicates of qRT-PCR were performed for each cDNA preparation.
545 To account for possible differences in cDNA synthesis and amplification efficiency, the data were
546 normalized to the transcript amount of *glyceraldehyde-3-phosphate dehydrogenase2* (*gapc2*).
547 Similar results were obtained when the data were normalized to the transcript amount of *EF-1a*.
548 Analysis of variance ($p \leq 0.01$) was applied separately to each of the two biological replicates and
549 statistical significance was considered only when reported for both replicates.

550

551 **ChIP assay**

552

553 Chromatin preparation was performed using frozen tissues according to the protocol
554 described by Luo et al., (2013), which was adapted for maize and teosinte plants. ChIP assays were
555 carried out as described by Locatelli et al., (2009) with minor modifications (see Supplemental

556 Materials and Methods for details regarding the protocol). The following antibodies were used: 6 µg
557 of α -H3ac (Millipore; 07-352), 10 µg of α -H3K4me2 (Millipore; 07-030); 4 µg of α -H3K4me3
558 (Active Motif; 39159), 10 µg of α -H3K36me2 (Millipore; 07-369), 12 µg of α -H3K27me3
559 (Millipore; 07-449) and 4 µg of α -H3C-ter (Abcam; ab1791). A no-antibody negative control was
560 performed by adding no antibody during incubation. Two independent ChIP experiments were
561 performed and qPCR and statistical analysis (analysis of variance, $p \leq 0.01$) were carried out as
562 described by Rossi et al. (2007). The sequences of primers used for ChIP assays are reported in
563 Supplemental Table S5.

564

565 **DNA methylation analysis**

566

567 Digestion with MspJI (New England Biolabs) was performed following the manufacturer's
568 instruction. Two independent MspJI treatments and three repetitions of qPCR analysis were carried
569 out and statistical analysis was performed as described by Locatelli et al., (2009). Genomic DNA
570 bisulfite treatment was performed with the EZ DNA Methylation kit (Zymo Research,) following
571 manufacturer's instructions. Primers for the mC analysis of the upper strand were designed using
572 the Kismeth web-based tool (<http://katahdin.mssm.edu/kismeth/revpage.pl>; Gruntman et al., 2008;
573 see Supplemental Table S5). One microliter of bisulfite treated DNA was used for PCR under the
574 following conditions: 1.5 mM MgCl₂, 0.2 mM of each dNTPs, 0.4 µM of each primer, and 1.25
575 units of Taq Platinum (Life Technologies). The PCR program was: 5 min 95 °C, 40 cycles of 30 sec
576 95 °C – 1 min 45 °C – 1 min 72 °C, 10 min 72 °C, and forever 4 °C. Amplified fragments were
577 cloned and ten independent clones were sequenced for each fragment.

578

579 **Accession Numbers**

580 The GenBank accession numbers of the genes cited in this study are: B73 *ZCN7*: KP202720
581 (*GRMZM2G141756*); B73 *ZCN8*: EU241899 (*GRMZM2G179264*); teosinte *ZCN7*: KP172200;
582 teosinte *ZCN8*: KP172201; B73 *id1*: GRMZM2G011357; B73 *gapc2*: U45855; B73 *EF1- α* :
583 U76259. Among parenthesis is reported the number of the gene model according the B73 maize
584 sequencing project (<http://www.maizegdb.org/>).

585

586 **Supplemental Data**

587

588 The following materials are available in the on-line version of this article.

589

590 **Supplemental Figure S1.** Schematic depiction of *ZCN7* and *ZCN8* genes and transcripts of maize
591 B73 inbred.

592

593 **Supplemental Figure S2.** Examination of *ZCN7/ZCN8* in plants at pre-transition (V4), transition
594 (V6), and post-transition reproductive stage (V8).

595

596 **Supplemental Figure S3.** Sampling strategy.

597

598 **Supplemental Figure S4.** Nucleotide sequence of *ZCN7* and *ZCN8* antisense RNA strand.

599

600 **Supplemental Figure S5.** Comparison of *ZCN7* and *ZCN8* transcript isoforms level in B73 and
601 teosinte plants under inductive floral conditions.

602

603 **Supplemental Figure S6.** Analysis of *ZCN7* histone modifications in B73 wild-type and *id1*
604 mutant plants.

605

606 **Supplemental Figure S7.** Analysis of *ZCN7* histone modifications in teosinte SD and NB plants.

607

608 **Supplemental Figure S8.** Analysis of mC level at *ZCN7* and *ZCN8* by MspJI restriction.

609

610 **Supplemental Figure S9.** Bisulfite sequencing analysis of mC at B73 *ZCN7*.

611

612 **Supplemental Figure S10.** Bisulfite sequencing analysis of mC at B73 *ZCN8*.

613

614 **Supplemental Figure S11.** Bisulfite sequencing analysis of mC at teosinte *ZCN7*.

615

616 **Supplemental Figure S12.** Bisulfite sequencing analysis of mC at teosinte *ZCN8*.

617

618 **Supplemental Table S1.** Sequence similarity of B73 and teosinte *ZCN7* and *ZCN8* genes.

619

620 **Supplemental Table S2.** *ZCN7* and *ZCN8* transcript levels obtained from RNA-seq experiments
621 using different B73 tissues.

622

623 **Supplemental Table S3.** Analysis of the mC profile of *ZCN7* and *ZCN8* by bisulfite sequencing.

624

625 **Supplemental Table S4.** List of primers used for B73 and teosinte cDNA synthesis in strand-
626 specific reverse transcription.

627

628 **Supplemental Table S5.** List of primers used in PCR.

629

630 **Supplemental Materials and Methods Online.**

631

632 **AKNOWLEDGMENTS**

633 We thank Fabio Fornara, Massimiliano Lauria, Lewis Lukens and Steven Rothstein for
634 critical reading of the manuscript. We are grateful to Raul Pirona for *in silico* reconstitution of the
635 teosinte genomic sequences and to Michael Mucci and Tannis Slimmon for providing expert plant
636 care at the Guelph Phytotron.

637

638 **AUTHOR CONTRIBUTIONS**

639 J.C. and V.R. conceived and designed research. I.M., K.T., R.S.B., A.H., J.C., and V.R.
640 performed research. I.M. and V.R. analyzed data. J.C. and V.R. wrote the article.

641

642 **FIGURES LEGENDS**

643

644 **Figure 1.** Photographs of B73 maize and teosinte plants induced and uninduced for flowering. A,
645 Wild type plant at V7 stage; inset shows meristem at floral transition stage. B, Maize *id1* mutant
646 plant at V7 stage; inset shows meristem at vegetative stage. C, Teosinte grown under NB for 27
647 days and induced for 10 days under SD conditions; inset shows inflorescence meristem. D, Teosinte
648 plant grown under non-inductive NB conditions for 37 days; inset shows uninduced meristem.
649 Teosinte plants exhibited extensive tillering, but only leaves from the main shoot were harvested for
650 analysis. Scale bar for all inset photos is 0.25 mm.

651

652 **Figure 2.** RT-PCR analysis of *ZCN7* and *ZCN8* transcripts in B73 and teosinte plants. A, RT-PCR
653 was performed with oligo(dT)-primed cDNA prepared with RNA extracted from mature (ML) and
654 immature (IL) leaves and with (+) or without (-) addition of reverse transcriptase (RT).
655 Schematization of *ZCN7* and *ZCN8* genes and position of primers used for RT-PCR are reported.
656 The structure of both genes is conserved in B73 and teosinte. B, Strand-specific RT-PCR carried
657 out using forward (*ZCN7*-for and *ZCN8*-for) and reverse (*ZCN7*-rev and *ZCN8*-rev) primers for
658 synthesizing cDNA produced by the antisense and sense RNA strand, respectively. Subsequent RT-
659 PCR with *ZCN7/8*-1 and *ZCN7/8*-2 primers permits the detection of both spliced and unspliced
660 RNAs. C, Diagram schematizing the three transcript isoforms produced by *ZCN7* and *ZCN8* genes.
661 RNAs length and position with respect to the gene structure is based on strand-specific RT-PCR
662 results with B73 plants.

663

664 **Figure 3.** Strand-specific qRT-PCR analysis of *ZCN7* and *ZCN8* transcript isoforms in B73 and
665 teosinte plants. Real-time qRT-PCR quantification of *ZCN7* and *ZCN8* sense and antisense
666 transcripts from mature (ML) and immature (IL) leaves of wild-type (wt) and *id1* mutant B73 plants
667 (A) and of teosinte plants grown under inductive short days (SD) and inhibitory night breaks (NB)
668 flowering conditions (B). Bar diagrams are the mean value of transcript amount for one biological
669 replicate, normalized to *gapc2* sense mRNA. The value of wt and SD is set to 1 and the amount and
670 direction (increase or decrease) of change for each RNA isoform in *id1* mutants vs wt (A) or in SD
671 vs NB conditions (B) was calculated using the $2^{-\Delta\Delta Ct}$ method (for value < 1 the negative value was
672 obtained by applying the formula $-1/2^{-\Delta\Delta Ct}$). Asterisk indicates statistically significant change ($p \leq$
673 0.01) when it was achieved in the separate analysis of the two biological replicates.

674

675 **Figure 4.** Analysis of *ZCN8* histone modifications in B73 wild-type and *id1* mutant plants. A,
676 Schematic depiction of *ZCN8* gene, with black boxes representing exons. Positions of the regions
677 analyzed in ChIP assays are indicated. B, Bar diagrams represent real-time PCR quantification of
678 ChIP DNA, reported as percentage of the chromatin input, from assays performed using the
679 indicated antibodies. The data are average values from two independent ChIP assays and from three
680 PCR repetitions for each ChIP assay and are reported by subtracting the background signal,
681 measured by omitting antibody during the ChIP procedure. Asterisk indicates statistically
682 significant change ($p \leq 0.01$) in *id1* mutant vs wild-type. The grouping of histone marks on the basis
683 of how its variation associates with activity of *id1* gene is indicated by parentheses. Similar results
684 were obtained after correction for nucleosome occupancy measured as reported by Rossi et al.,
685 (2007).

686

687 **Figure 5.** Analysis of *ZCN8* histone modifications in teosinte SD and NB plants. A, Schematic
688 depiction of *ZCN8* gene, with black boxes representing exons. Positions of the regions analyzed in
689 ChIP assays are indicated. B, Bar diagrams represent real-time PCR quantification of ChIP DNA,
690 reported as percentage of chromatin input, from assays using the indicated antibodies. The data are
691 average values from two independent ChIP assays and from three PCR repetitions for each ChIP
692 assay and are reported by subtracting the background signal, measured by omitting antibody during
693 the ChIP procedure. Asterisk indicates statistically significant change ($p \leq 0.01$) in SD vs NB
694 plants. The grouping of histone marks on the basis of how its variation associates with SD floral
695 induction is indicated by parentheses. Similar results were obtained after correction for nucleosome
696 occupancy measured as reported by Rossi et al., (2007).

697

698 **Figure 6.** Summary of *ZCN7* and *ZCN8* epigenetic pattern variation in B73 and teosinte plants. The
699 diagram is based on data reported in Figures 4 and 5 and in Supplemental Figures S6 and S7. The
700 direction of the arrow indicates the direction of the change for the histone modification listed on the
701 left of the figure and for cytosine methylation measured by means of restriction with MspJI enzyme.
702 Variation of epigenetic mark levels that occur in immature leaf and is maintained in mature leaf is
703 highlighted by black arrows.

704

705 **Figure 7.** Model of florigen regulation in autonomous maize and photoperiod-induced teosinte.
706 Autonomous maize (left) requires ID1 regulatory protein activity (orange stars) in developing
707 leaves to establish chromatin modifications that allow expression of florigen genes (*ZCN7* and

708 *ZCN8*). Thus *id1* gene acts in immature leaves to establish a chromatin signature and prime the leaf
709 for florigen synthesis as the leaf develops. Active chromatin is specified by acetylated histone H3
710 (H3ac). Once the distal portion of the leaf develops, another signal (unknown) activates florigen
711 production in leaf vasculature, which then migrates to the shoot apical meristem (SAM) to activate
712 flowering genes (purple dotted line). The autonomous signal may consist, partly, in changes in
713 metabolic activity. Metabolic changes could also indirectly activate florigen production (question
714 mark). In teosinte (right) floral induction is dependent on SD photoperiods and the circadian clock
715 to activate florigen production. Similar to *id1*, the photoperiod pathway also establishes chromatin
716 modifications in immature leaves, which enable florigen synthesis in mature leaves, but the pattern
717 of histone modifications related to its activity is different from the one created by *id1* in the
718 autonomous pathway; i.e. open chromatin is specified by H3K4me2/me3. The horizontal dashed
719 line across the mature maize and teosinte leaves delineates the regions of the immature, developing
720 leaf zone (lower) from the mature leaf blade (upper).

721

722 LITERATURE CITED

723

- 724 Abe M, Kobayashi Y, Yamamoto S, Daimon Y, Yamaguchi A, Ikeda Y, Ichinoki H, Notaguchi M, Goto K, Araki T
725 (2005) FD, a bZIP protein mediating signals from the floral pathway integrator FT at the shoot apex. *Science*
726 309: 1052–1056
- 727 Adrian J, Farrona S, Reimer JJ, Albani MC, Coupland G, Turck F (2010) Cis-regulatory elements and
728 chromatin state coordinately control temporal and spatial expression of FLOWERING LOCUS T in
729 Arabidopsis. *Plant Cell* 22: 1425–1440
- 730 Andres F, Coupland G (2012) The genetic basis of flowering responses to seasonal cues. *Nat Rev Genet* 13:
731 627–639
- 732 Bannister AJ, Kouzarides T (2011) Regulation of chromatin by histone modifications. *Cell Res* 21: 381–395
- 733 Bouchet S, Servin B, Bertin P, Madur D, Combes V, Dumas F, Brunel D, Laborde J, Charcosset A, Nicolas S
734 (2013) Adaptation of maize to temperate climates: mid-density genome-wide association genetics and
735 diversity patterns reveal key genomic regions, with a major contribution of the Vgt2 (ZCN8) locus. *PLoS One*
736 8: e71377
- 737 Bu Z, Yu Y, Li Z, Liu Y, Jiang W, Huang Y, Dong AW (2014) Regulation of Arabidopsis flowering by the histone
738 mark readers MRG1/2 via interaction with CONSTANS to modulate FT expression. *PLoS Genet* 10: e1004617
- 739 Chailakhyan MK (1937) Concerning the hormonal nature of plant development processes. *Dokl Akad Nauk*
740 SSSR 16: 227–230
- 741 Cohen-Karni D, Xu D, Apone L, Fomenkov A, Sun Z, Davis PJ, Kinney SR, Yamada-Mabuchi M, Xu SY, Davis T,
742 Pradhan S, Roberts RJ, Zheng Y (2011) The MspJI family of modification-dependent restriction
743 endonucleases for epigenetic studies. *Proc Nat Acad Science USA* 108: 11040–11045
- 744 Colasanti J, Coneva V (2009) Mechanisms of floral induction in grasses: something borrowed something
745 new. *Plant Physiol* 149: 56–62
- 746 Colasanti J, Muszynski MG (2009) The Maize Floral Transition. In SC Hake, JL Bennetzen, eds, *Handbook of*
747 *Maize: Its Biology*, Vol 1. Springer Science, New York, pp: 41–55
- 748 Colasanti J, Yuan Z, Sundaresan V (1998) The *indeterminate* gene encodes a zinc finger protein and
749 regulates a leaf-generated signal required for the transition to flowering in maize. *Cell* 93: 593–603
- 750 Coneva V, Zhu T, Colasanti J (2007) Expression differences between normal and *indeterminate1* maize
751 suggest downstream targets of ID1, a floral transition regulator in maize. *J Exp Bot* 58: 3679–3693
- 752 Coneva V, Guevara D, Rothstein SJ, Colasanti J (2012) Transcript and metabolite signature of maize source
753 leaves suggests a link between transitory starch to sucrose balance and the autonomous floral transition. *J*
754 *Exp Bot* 63: 5079–5092

- 755 Corbesier L, Vincent C, Jang S, Fornara F, Fan Q, Searle I, Giakountis A, Farrona, S, Gissot L, Turnbull C, et al
756 (2007) FT protein movement contributes to long-distance signaling in floral induction of Arabidopsis.
757 Science 316: 1030–1033
- 758 Danilevskaya ON, Meng X, Hou Z, Ananiev EV, Simmons CR (2008) A genomic and expression compendium
759 of the expanded PEBP gene family from maize. Plant Physiol 146: 250–264
- 760 De Lucia F, Dean C (2011) Long antisense transcripts and chromatin regulation. Curr Opin Plant Biol 14:
761 168–173
- 762 Finnegan EJ, Dennis ES (2007) Vernalization-induced trimethylation of histone H3 lysine 27 at FLC is not
763 maintained in mitotically quiescent cells. Curr Biol 17: 1978–1983
- 764 Giakountis A, Coupland G (2008) Phloem transport of flowering signals. Curr Opin Plant Biol 11: 687–694
- 765 Gruntman E, Qi Y, Slotkin RK, Roeder T, Martienssen RA, Sachidanandam R (2008) Kismeth: analyzer of
766 plant methylation states through bisulfite sequencing. BMC Bioinformatics 9: 371
- 767 Gu X, Wang Y, He Y (2013) Photoperiodic regulation of flowering time through periodic histone
768 deacetylation of the florigen gene FT. PLoS Biol 11: e1001649
- 769 He Y (2012) Chromatin regulation of flowering. Trends Plant Sci 17: 556–562
- 770 Henikoff S, Shilatifard A (2011) Histone modification: cause or cog? Trends Genet 27: 389–96
- 771 Jaeger KE, Wigge, PA (2007) FT protein acts as a long-range signal in Arabidopsis. Curr Biol 17: 1050–1054
- 772 Jiang D, Wang Y, Wang Y, He Y (2008) Repression of FLOWERING LOCUS C and FLOWERING LOCUS T by the
773 Arabidopsis Polycomb repressive complex 2 components. PLoS ONE 3: e3404
- 774 Kozaki A, Hake S, Colasanti J (2004) The maize ID1 flowering time regulator is a zinc finger protein with
775 novel DNA binding properties. Nucleic Acids Res 32: 1710–1720
- 776 Lauria M, Rossi V (2011) Epigenetic control of gene regulation in plants. Biochim Biophys Acta 1809: 369–
777 378
- 778 Lazakis CM, Coneva V, Colasanti J (2011) ZCN8 encodes a potential orthologue of Arabidopsis FT that
779 integrates both endogenous and photoperiod flowering signals in maize. J Exp Bot 62: 4833–4842
- 780 Locatelli S, Piatti P, Motto M, Rossi V (2009) Chromatin and DNA modifications in Opaque2-mediated
781 regulation of gene transcription during maize endosperm development. Plant Cell 21: 1410–1427
- 782 López-González L, Mouriz A, Narro-Diego L, Bustos R, Martínez-Zapater JM, Jarillo JA, Piñeiro M (2014)
783 Chromatin-dependent repression of the Arabidopsis floral integrator genes involves plant specific PHD-
784 containing proteins. Plant Cell 26: 3922–3938
- 785 Luo C, Sidote DJ, Zhang Y, Kerstetter RA, Michael TP, Lam E (2013) Integrative analysis of chromatin states
786 in Arabidopsis identified potential regulatory mechanisms for natural antisense transcript production. Plant
787 J 73: 77–90

- 788 Makarevitch I, Eichten SR, Briskine R, Waters AJ, Danilevskaya ON, Meeley RB, Myers CL, Vaughn MW,
789 Springer NM (2013) Genomic Distribution of Maize Facultative Heterochromatin Marked by Trimethylation
790 of H3K27. *Plant Cell* 25: 780-793
- 791 Mascheretti I, Battaglia R, Mainieri D, Altana A, Lauria M, Rossi V (2013) The WD40-repeat proteins NFC101
792 and NFC102 regulate different aspects of maize development through chromatin modification. *Plant Cell*
793 25: 404-420
- 794 Matsubara K, Yamanouchi U, Wang ZX, Minobe Y, Izawa T, Yano M (2008) Ehd2, a rice ortholog of the maize
795 INDETERMINATE1 gene, promotes flowering by up-regulating Ehd1. *Plant Physiol* 148: 1425-1435
- 796 Meng X, Muszynski MG, Danilevskaya ON (2011) The FT-like ZCN8 gene functions as a floral activator and is
797 involved in photoperiod sensitivity in maize. *Plant Cell* 23: 942-960
- 798 Miller TA, Muslin EH, Dorweiler JE (2008) A maize CONSTANS-like gene, conz1, exhibits distinct diurnal
799 expression patterns in varied photoperiods. *Planta* 227: 1377-1388
- 800 Muszynski MG, Dam T, Li B, Shirbroun DM, Hou ZL, Bruggemann E, Archibald R, Ananiev EV, Danilevskaya
801 ON (2006) Delayed flowering1 encodes a basic leucine zipper protein that mediates floral inductive signals
802 at the shoot apex in maize. *Plant Physiol* 142: 1523-1536
- 803 Park SJ, Kim SL, Lee S, Je BI, Piao HL, Park SH, Kim CM, Ryu, CH, Park SH, Xuan YH, et al (2008) Rice
804 Indeterminate 1 (OsId1) is necessary for the expression of Ehd1 (Early heading date 1) regardless of
805 photoperiod. *Plant J* 56: 1018-1029
- 806 Regulski M, Lu Z, Kendall J, Donoghue MT, Reinders J, Llaca V, Deschamps S, Smith A, Levy D, McCombie
807 WR, et al (2013) The maize methylome influences mRNA splice sites and reveals widespread paramutation-
808 like switches guided by small RNA. *Genome Res* 23: 1651-1662
- 809 Rossi V, Locatelli S, Varotto S, Donn G, Pirona R, Henderson DA, Hartings H, Motto M (2007) Maize histone
810 deacetylase *hda101* is involved in plant development, gene transcription, and sequence-specific
811 modulation of histone modification of genes and repeats. *Plant Cell* 19: 1145-1162
- 812 Samach A, Onouchi H, Gold SE, Ditta GS, Schwarz-Sommer Z, Yanofsky MF, Coupland G (2000) Distinct roles
813 of CONSTANS target genes in reproductive development of *Arabidopsis*. *Science* 288: 1613-1616
- 814 Sekhon RS, Briskine R, Hirsch CN, Myers CL, Springer NM, Buell CR, de Leon N, Kaepller SM (2013) Maize
815 gene atlas developed by RNA sequencing and comparative evaluation of transcriptomes based on RNA
816 sequencing and microarrays. *PLoS ONE* 8: e61005
- 817 Sun C, Fang J, Zhao T, Xu B, Zhang F, Liu L, Tang J, Zhang G, Deng X, Chen F, et al (2012) The histone
818 methyltransferase SDG724 mediates H3K36me2/3 deposition at MADS50 and RFT1 and promotes flowering
819 in rice. *Plant Cell* 24: 3235-3247
- 820 Tiwari SB, Shen Y, Chang H-C, Hou Y, Harris A, Ma SF, McPartland M, Hymus GJ, Adam L, Marion C, et al.
821 (2010) The flowering time regulator CONSTANS is recruited to the FLOWERING LOCUS T promoter via a
822 unique cis-element. *New Phytol* 187: 57-66

- 823 Turck F, Roudier F, Farrona S, Martin-Magniette ML, Guillaume E, Buisine N, Gagnot S, Martienssen RA,
824 Coupland G, Colot V (2007) Arabidopsis TFL2/LHP1 specifically associates with genes marked by
825 trimethylation of histone H3 lysine 27. *PLoS Genet* 3: e86
- 826 Turck F, Fornara F, Coupland G (2008) Regulation and identity of florigen: FLOWERING LOCUS T moves
827 center stage. *Annual Rev Plant Biol* 59: 573–594
- 828 Wang Y, Gu X, Yuan W, Schmitz RJ, He Y (2014) Photoperiodic control of the floral transition through a
829 distinct polycomb repressive complex. *Dev Cell* 28: 727–736
- 830 Wigge PA, Kim MC, Jaeger KE, Busch W, Schmid M, Lohmann JU, Weigel D (2005) Integration of spatial and
831 temporal information during floral induction in *Arabidopsis*. *Science* 309: 1056–1059
- 832 Wong AY, Colasanti J (2007) Maize floral regulator protein INDETERMINATE1 is localized to developing
833 leaves and is not altered by light or the sink/source transition. *J Exp Bot* 58: 403–414
- 834 Wu CY, You CJ, Li CS, Long T, Chen GX, Byrne ME, Zhang QF (2008) RID1, encoding a Cys2/His2-type zinc
835 finger transcription factor, acts as a master switch from vegetative to floral development in rice. *Proc Nat
836 Acad Science USA* 105: 12915–12920
- 837 Young MD, Willson TA, Wakefield MJ, Trounson E, Hilton DJ, Blewitt ME, Oshlack A, Majewski IJ (2011)
838 ChIP-seq analysis reveals distinct H3K27me3 profiles that correlate with transcriptional activity. *Nucleic
839 Acids Res* 39: 7415–7427
- 840

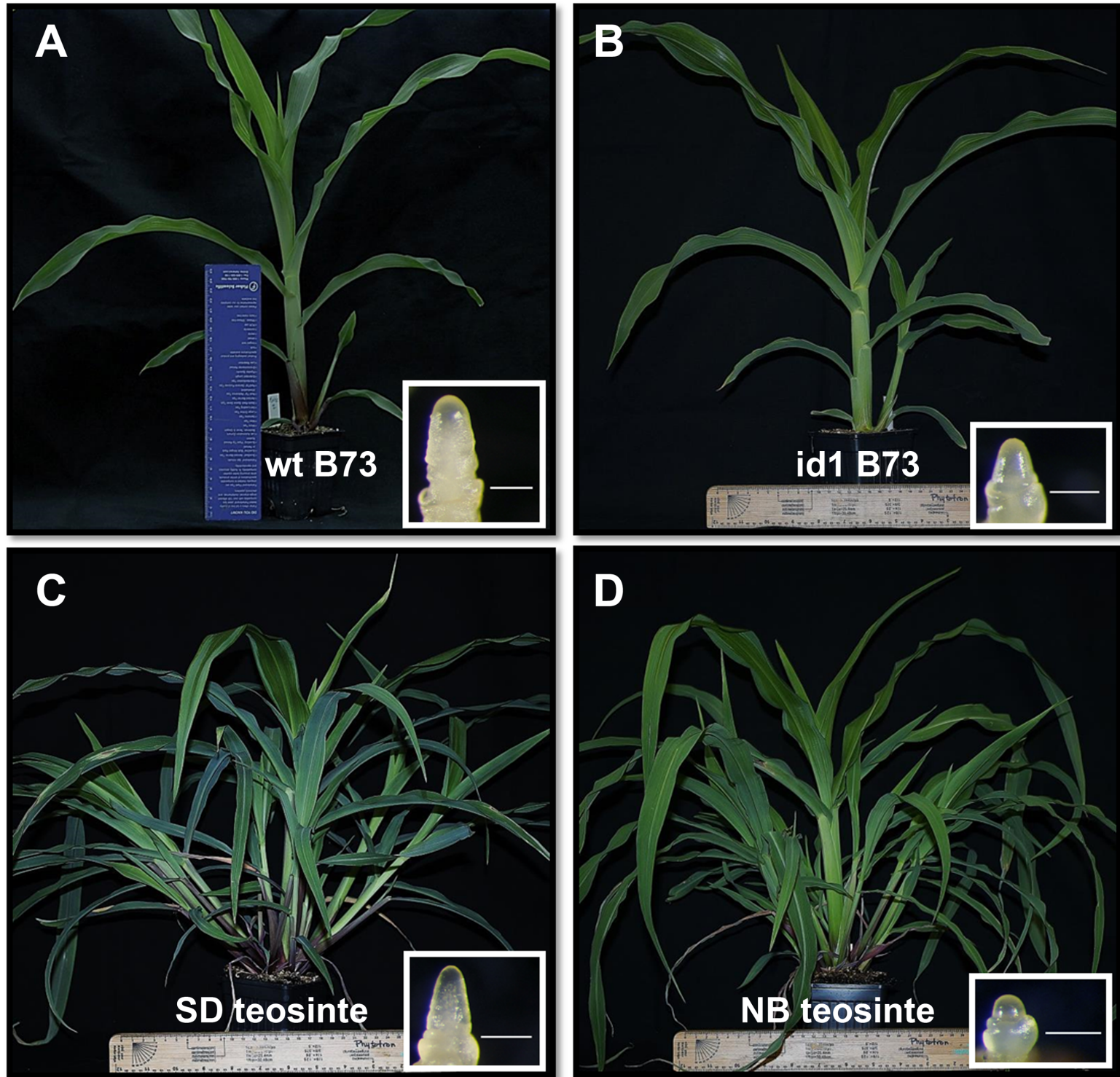


Figure 1. Photographs of B73 maize and teosinte plants induced and uninduced for flowering. A, Wild type plant at V7 stage; inset shows meristem at floral transition stage. B, Maize *id1* mutant plant at V7 stage; inset shows meristem at vegetative stage. C, Teosinte grown under NB for 27 days and induced for 10 days under SD conditions; inset shows inflorescence meristem. D, Teosinte plant grown under non-inductive NB conditions for 37 days; inset shows uninduced meristem. Teosinte plants exhibited extensive tillering, but only leaves from the main shoot were harvested for analysis. Scale bar for all inset photos is 0.25 mm.

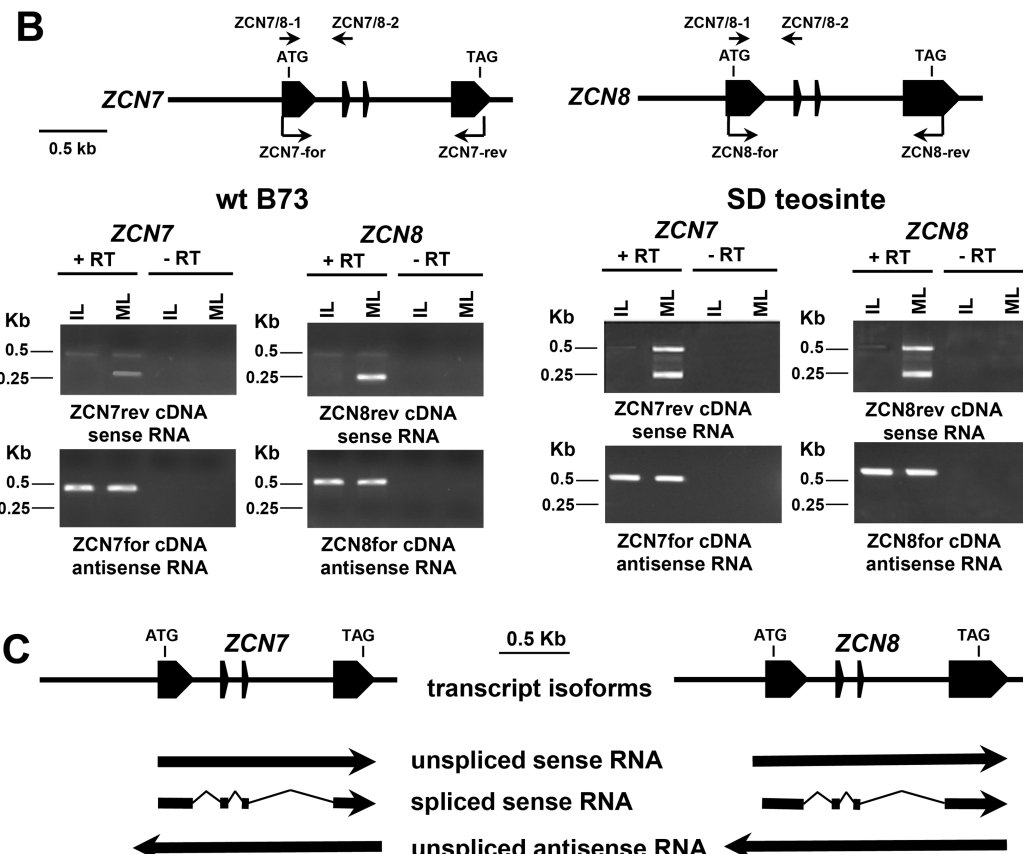
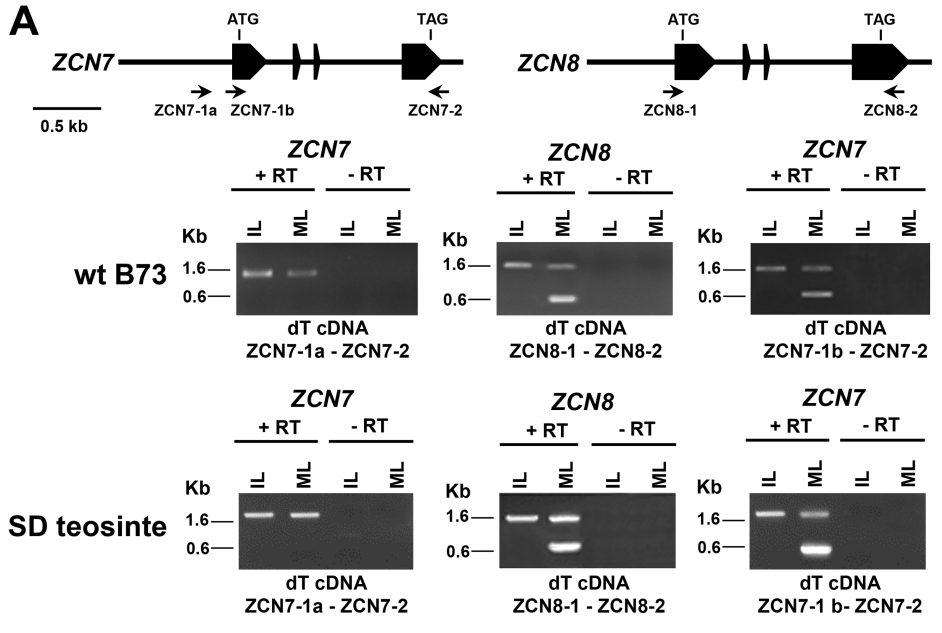
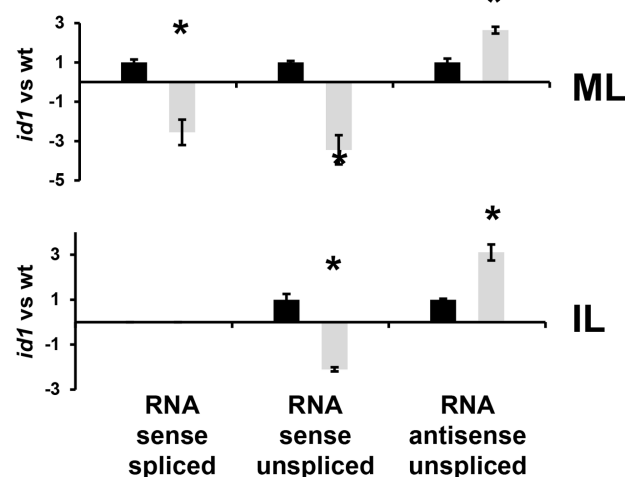
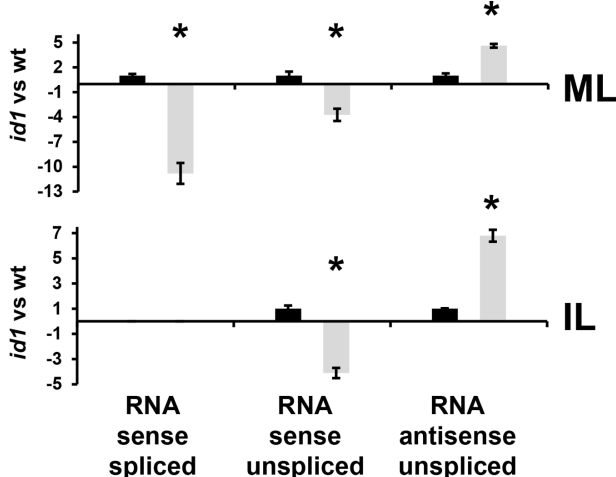


Figure 2. RT-PCR analysis of *ZCN7* and *ZCN8* transcripts in B73 and teosinte plants. A, RT-PCR was performed with oligo(dT)-primed cDNA prepared with RNA extracted from mature (ML) and immature (IL) leaves and with (+) or without (-) addition of reverse transcriptase (RT). Schematization of *ZCN7* and *ZCN8* genes and position of primers used for RT-PCR are reported. The structure of both genes is conserved in B73 and teosinte. B, Strand-specific RT-PCR carried out using forward (*ZCN7*-for and *ZCN8*-for) and reverse (*ZCN7*-rev and *ZCN8*-rev) primers for synthesizing cDNA produced by the antisense and sense RNA strand, respectively. Subsequent RT-PCR with *ZCN7*/8-1 and *ZCN7*/8-2 primers permits the detection of both spliced and unspliced RNAs. C, Diagram schematizing the three transcript isoforms produced by *ZCN7* and *ZCN8* genes. RNAs length and position with respect to the gene structure is based on strand-specific RT-PCR results with B73 plants.

A**B73**■ wt ■ *id1***ZCN7****ZCN8****B****teosinte**

■ SD ■ NB

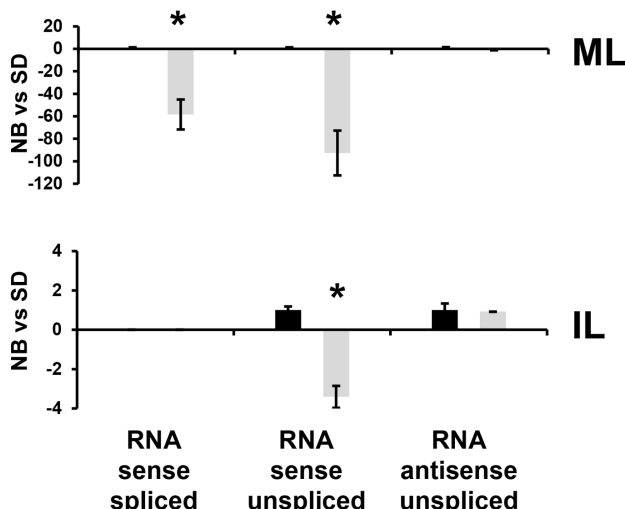
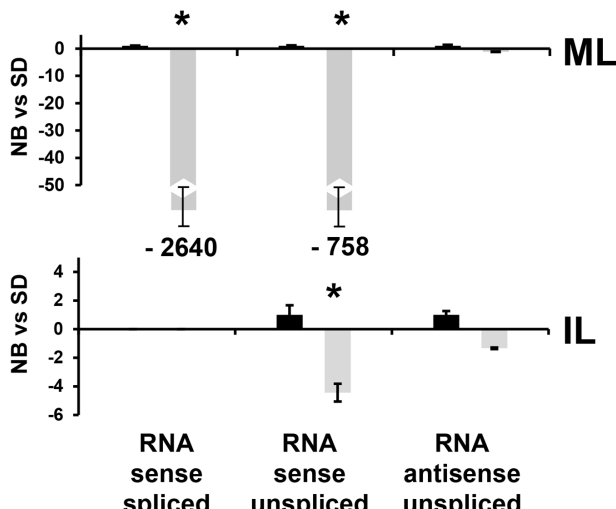
ZCN7**ZCN8**

Figure 3. Strand-specific qRT-PCR analysis of *ZCN7* and *ZCN8* transcript isoforms in B73 and teosinte plants. Real-time qRT-PCR quantification of *ZCN7* and *ZCN8* sense and antisense transcripts from mature (ML) and immature (IL) leaves of wild-type (wt) and *id1* mutant B73 plants (A) and of teosinte plants grown under inductive short days (SD) and inhibitory night breaks (NB) flowering conditions (B). Bar diagrams are the mean value of transcript amount for one biological replicate, normalized to *gapc2* sense mRNA. The value of wt and SD is set to 1 and the amount and direction (increase or decrease) of change for each RNA isoform in *id1* mutants vs wt (A) or in SD vs NB conditions (B) was calculated using the $2^{-\Delta\Delta Ct}$ method (for value < 1 the negative value was obtained by applying the formula $-1/2^{-\Delta\Delta Ct}$). Asterisk indicates statistically significant change ($p < 0.01$) when it was achieved in the separate analysis of the two biological replicates.

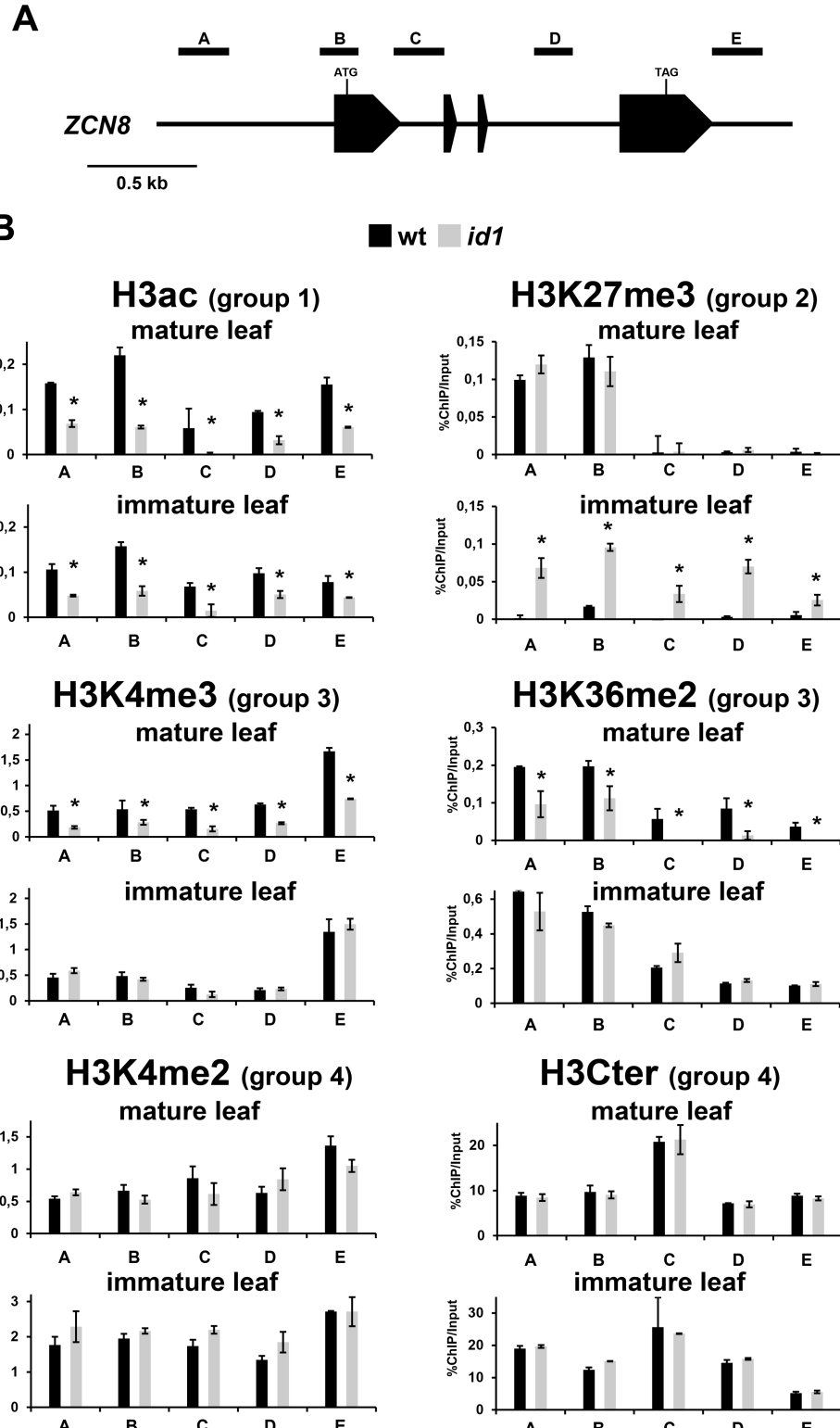


Figure 4. Analysis of ZCN8 histone modifications in B73 wild-type and *id1* mutant plants. A, Schematic depiction of ZCN8 gene, with black boxes representing exons. Positions of the regions analyzed in ChIP assays are indicated. B, Bar diagrams represent real-time PCR quantification of ChIP DNA, reported as percentage of the chromatin input, from assays performed using the indicated antibodies. The data are average values from two independent ChIP assays and from three PCR repetitions for each ChIP assay and are reported by subtracting the background signal, measured by omitting antibody during the ChIP procedure. Asterisk indicates statistically significant change ($p \leq 0.01$) in *id1* mutant vs wild-type. The grouping of histone marks on the basis of how its variation associates with activity of *id1* gene is indicated by parentheses. Similar results were obtained after correction for nucleosome occupancy measured as reported by Rossi et al., (2007).

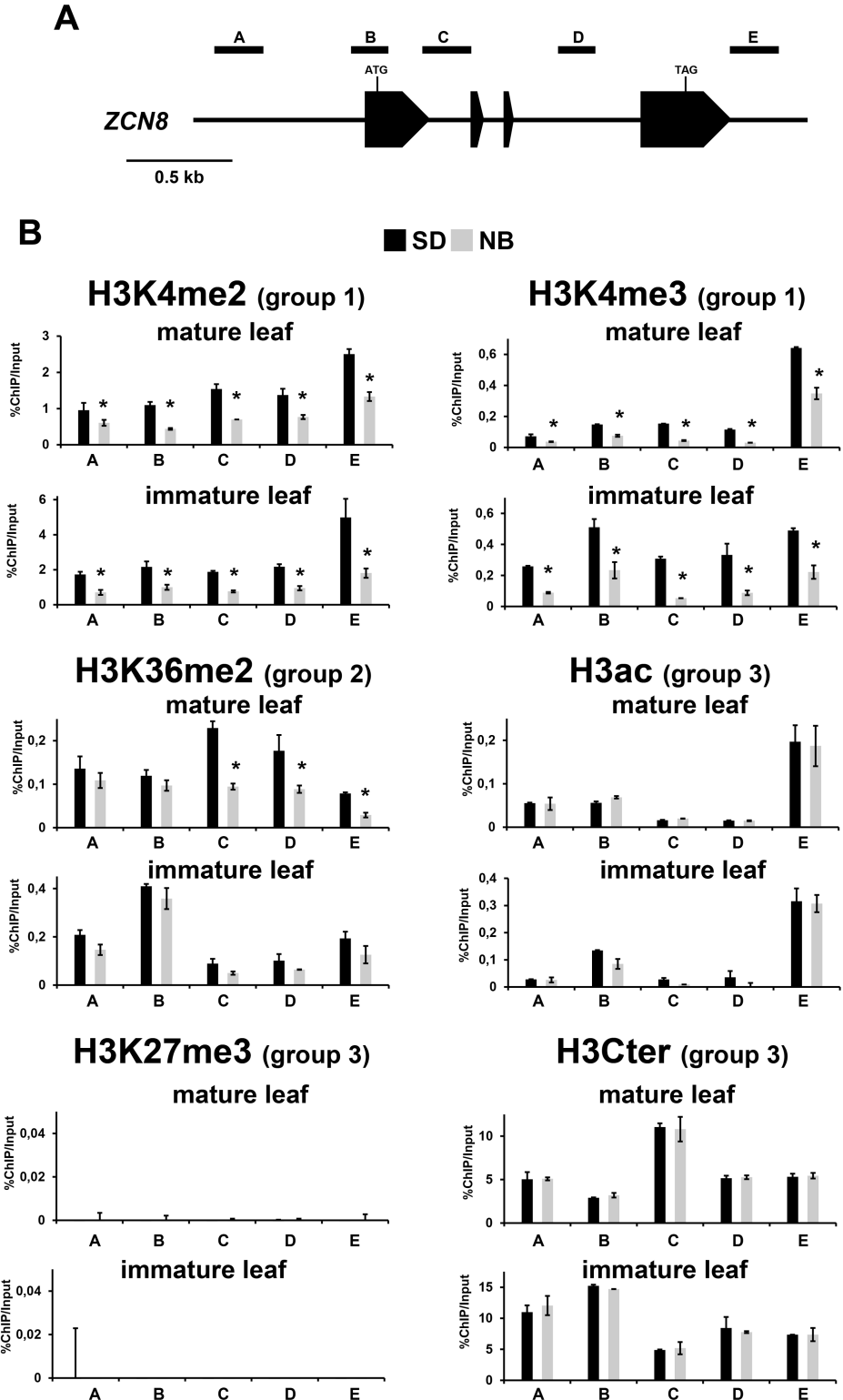


Figure 5. Analysis of *ZCN8* histone modifications in teosinte SD and NB plants. A, Schematic depiction of *ZCN8* gene, with black boxes representing exons. Positions of the regions analyzed in ChIP assays are indicated. B, Bar diagrams represent real-time PCR quantification of ChIP DNA, reported as percentage of chromatin input, from assays using the indicated antibodies. The data are average values from two independent ChIP assays and from three PCR repetitions for each ChIP assay and are reported by subtracting the background signal, measured by omitting antibody during the ChIP procedure. Asterisk indicates statistically significant change ($p \leq 0.01$) in SD vs NB plants. The grouping of histone marks on the basis of how its variation associates with SD floral induction is indicated by parentheses. Similar results were obtained after correction for nucleosome occupancy measured as reported by Rossi et al., (2007).

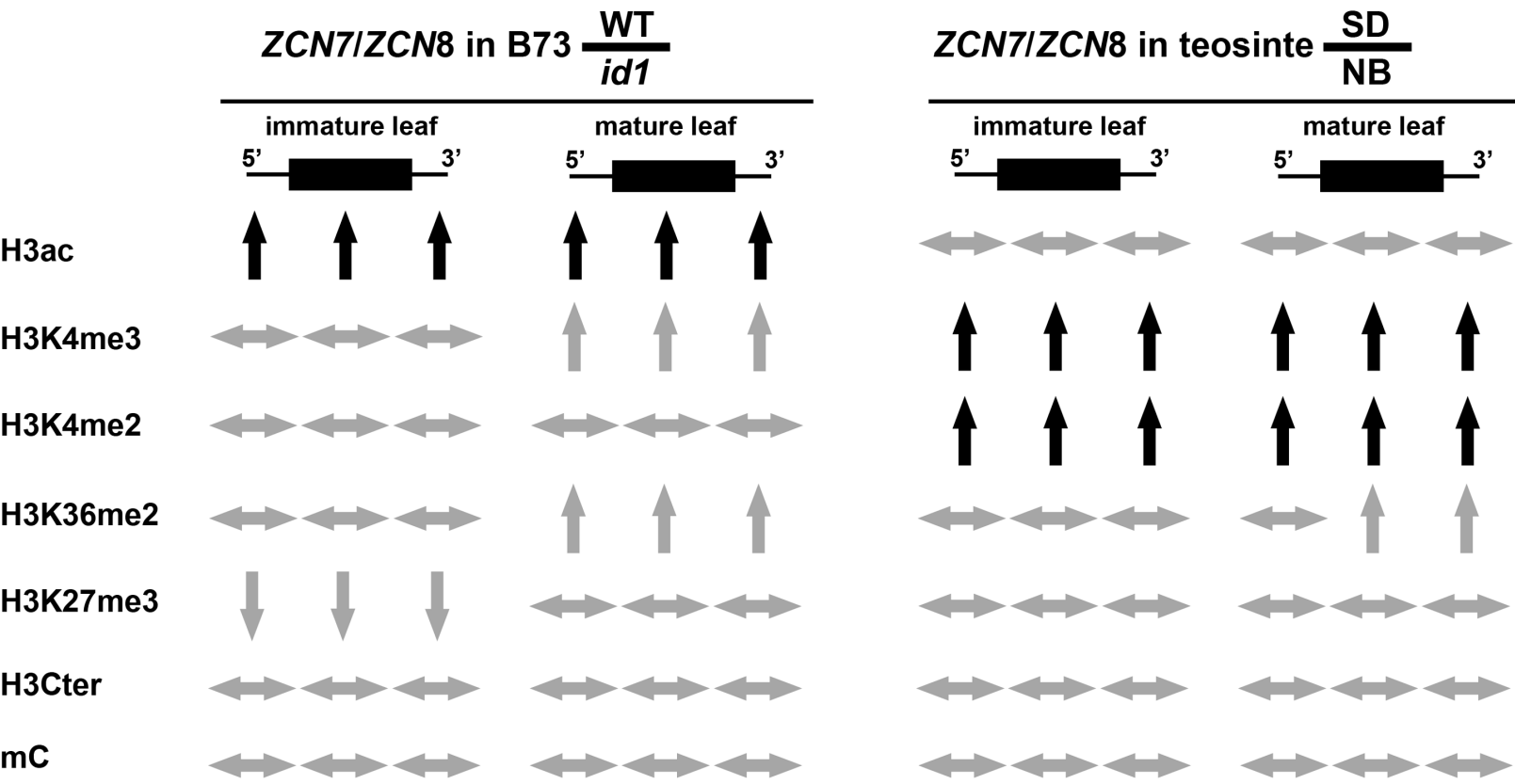


Figure 6. Summary of *ZCN7* and *ZCN8* epigenetic pattern variation in B73 and teosinte plants. The diagram is based on data reported in Figures 4 and 5 and in Supplemental Figures S6 and S7. The direction of the arrow indicates the direction of the change for the histone modification listed on the left of the figure and for cytosine methylation measured by means of restriction with MspJI enzyme. Variation of epigenetic mark levels that occur in immature leaf and is maintained in mature leaf is highlighted by black arrows.

AUTONOMOUS FLOWERING
TEMPERATE MAIZE

PHOTOPERIOD-DEPENDENT
TROPICAL MAIZE

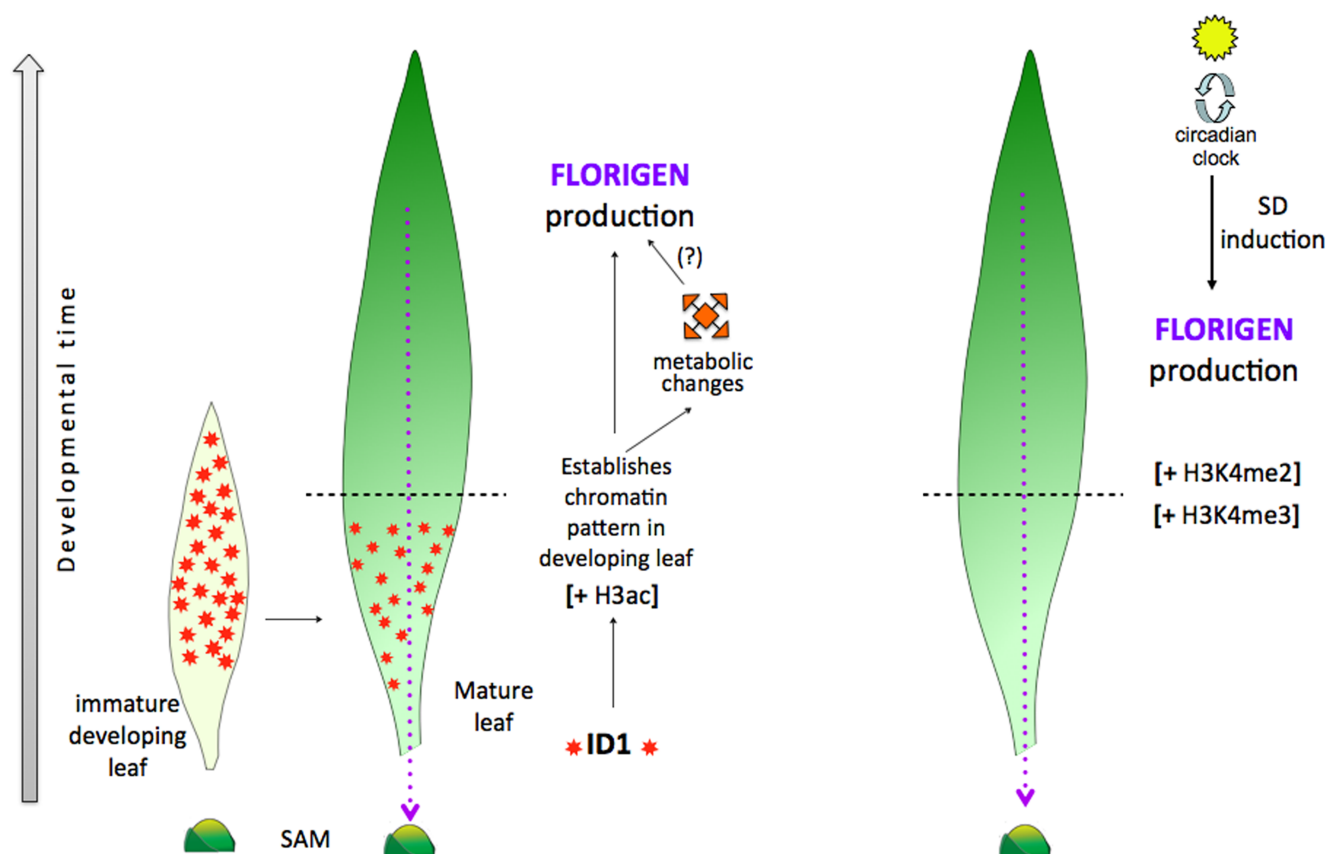


Figure 7. Model of florigen regulation in autonomous maize and photoperiod-induced teosinte. Autonomous maize (left) requires ID1 regulatory protein activity (orange stars) in developing leaves to establish chromatin modifications that allow expression of florigen genes (*ZCN7* and *ZCN8*). Thus *id1* gene acts in immature leaves to establish a chromatin signature and prime the leaf for florigen synthesis as the leaf develops. Active chromatin is specified by acetylated histone H3 (H3ac). Once the distal portion of the leaf develops, another signal (unknown) activates florigen production in leaf vasculature, which then migrates to the shoot apical meristem (SAM) to activate flowering genes (purple dotted line). The autonomous signal may consist, partly, in changes in metabolic activity. Metabolic changes could also indirectly activate florigen production (question mark). In teosinte (right) floral induction is dependent on SD photoperiods and the circadian clock to activate florigen production. Similar to *id1*, the photoperiod pathway also establishes chromatin modifications in immature leaves, which enable florigen synthesis in mature leaves, but the pattern of histone modifications related to its activity is different from the one created by *id1* in the autonomous pathway; i.e. open chromatin is specified by H3K4me2/me3. The horizontal dashed line across the mature maize and teosinte leaf separates the regions of the immature, developing leaf zone (lower) from the mature leaf blade (upper).

Parsed Citations

Abe M, Kobayashi Y, Yamamoto S, Daimon Y, Yamaguchi A, Ikeda Y, Ichinoki H, Notaguchi M, Goto K, Araki T (2005) FD, a bZIP protein mediating signals from the floral pathway integrator FT at the shoot apex. *Science* 309: 1052-1056

Pubmed: [Author and Title](#)

CrossRef: [Author and Title](#)

Google Scholar: [Author Only Title Only Author and Title](#)

Adrian J, Farrona S, Reimer JJ, Albani MC, Coupland G, Turck F (2010) Cis-regulatory elements and chromatin state coordinately control temporal and spatial expression of FLOWERING LOCUS T in *Arabidopsis*. *Plant Cell* 22: 1425-1440

Pubmed: [Author and Title](#)

CrossRef: [Author and Title](#)

Google Scholar: [Author Only Title Only Author and Title](#)

Andres F, Coupland G (2012) The genetic basis of flowering responses to seasonal cues. *Nat Rev Genet* 13: 627-639

Pubmed: [Author and Title](#)

CrossRef: [Author and Title](#)

Google Scholar: [Author Only Title Only Author and Title](#)

Bannister AJ, Kouzarides T (2011) Regulation of chromatin by histone modifications. *Cell Res* 21: 381-395

Pubmed: [Author and Title](#)

CrossRef: [Author and Title](#)

Google Scholar: [Author Only Title Only Author and Title](#)

Bouchet S, Servin B, Bertin P, Madur D, Combes V, Dumas F, Brunel D, Laborde J, Charcosset A, Nicolas S (2013) Adaptation of maize to temperate climates: mid-density genome-wide association genetics and diversity patterns reveal key genomic regions, with a major contribution of the Vgt2 (ZCN8) locus. *PLoS One* 8: e71377

Pubmed: [Author and Title](#)

CrossRef: [Author and Title](#)

Google Scholar: [Author Only Title Only Author and Title](#)

Bu Z, Yu Y, Li Z, Liu Y, Jiang W, Huang Y, Dong AW (2014) Regulation of *Arabidopsis* flowering by the histone mark readers MRG1/2 via interaction with CONSTANS to modulate FT expression. *PLoS Genet* 10: e1004617

Pubmed: [Author and Title](#)

CrossRef: [Author and Title](#)

Google Scholar: [Author Only Title Only Author and Title](#)

Chailakhyan MK (1937) Concerning the hormonal nature of plant development processes. *Dokl Akad Nauk SSSR* 16: 227-230

Pubmed: [Author and Title](#)

CrossRef: [Author and Title](#)

Google Scholar: [Author Only Title Only Author and Title](#)

Cohen-Karni D, Xu D, Apone L, Fomenkov A, Sun Z, Davis PJ, Kinney SR, Yamada-Mabuchi M, Xu SY, Davis T, Pradhan S, Roberts RJ, Zheng Y (2011) The MspJI family of modification-dependent restriction endonucleases for epigenetic studies. *Proc Nat Acad Science USA* 108: 11040-11045

Pubmed: [Author and Title](#)

CrossRef: [Author and Title](#)

Google Scholar: [Author Only Title Only Author and Title](#)

Colasanti J, Coneva V (2009) Mechanisms of floral induction in grasses: something borrowed something new. *Plant Physiol* 149: 56-62

Pubmed: [Author and Title](#)

CrossRef: [Author and Title](#)

Google Scholar: [Author Only Title Only Author and Title](#)

Colasanti J, Muszynski MG (2009) The Maize Floral Transition. In SC Hake, JL Bennetzen, eds, *Handbook of Maize: Its Biology*, Vol 1. Springer Science, New York, pp: 41-55

Pubmed: [Author and Title](#)

CrossRef: [Author and Title](#)

Google Scholar: [Author Only Title Only Author and Title](#)

Colasanti J, Yuan Z, Sundaresan V (1998) The *indeterminate* gene encodes a zinc finger protein and regulates a leaf-generated signal required for the transition to flowering in maize. *Cell* 93: 593-603

Pubmed: [Author and Title](#)

CrossRef: [Author and Title](#)

Google Scholar: [Author Only Title Only Author and Title](#)

Coneva V, Zhu T, Colasanti J (2007) Expression differences between normal and *indeterminate1* maize suggest downstream targets of ID1, a floral transition regulator in maize. *J Exp Bot* 58: 3679-3693

Pubmed: [Author and Title](#)

CrossRef: [Author and Title](#)

Google Scholar: [Author Only Title Only Author and Title](#)

Coneva V, Guevara D, Rothstein SJ, Colasanti J (2012) Transcript and metabolite signature of maize source leaves suggests a link between transitory starch to sucrose balance and the autonomous floral transition. *J Exp Bot* 63: 5079-5092

Pubmed: [Author and Title](#)

CrossRef: [Author and Title](#)

Google Scholar: [Author Only Title Only Author and Title](#)

Corbesier L, Vincent C, Jang S, Endara F, Fan Q, Steward G, Giakountis A, Farrona S, Ghislain P, Turnbull C, et al (2007) FT protein

Copyright © 2015 American Society of Plant Biologists. All rights reserved.

movement contributes to long-distance signaling in floral induction of *Arabidopsis*. *Science* 316: 1030-1033

Pubmed: [Author and Title](#)

CrossRef: [Author and Title](#)

Google Scholar: [Author Only Title Only Author and Title](#)

Danilevskaya ON, Meng X, Hou Z, Ananiev EV, Simmons CR (2008) A genomic and expression compendium of the expanded PEBP gene family from maize. *Plant Physiol* 146: 250-264

Pubmed: [Author and Title](#)

CrossRef: [Author and Title](#)

Google Scholar: [Author Only Title Only Author and Title](#)

De Lucia F, Dean C (2011) Long antisense transcripts and chromatin regulation. *Curr Opin Plant Biol* 14: 168-173

Pubmed: [Author and Title](#)

CrossRef: [Author and Title](#)

Google Scholar: [Author Only Title Only Author and Title](#)

Finnegan EJ, Dennis ES (2007) Vernalization-induced trimethylation of histone H3 lysine 27 at FLC is not maintained in mitotically quiescent cells. *Curr Biol* 17: 1978-1983

Pubmed: [Author and Title](#)

CrossRef: [Author and Title](#)

Google Scholar: [Author Only Title Only Author and Title](#)

Giakountis A, Coupland G (2008) Phloem transport of flowering signals. *Curr Opin Plant Biol* 11: 687-694

Pubmed: [Author and Title](#)

CrossRef: [Author and Title](#)

Google Scholar: [Author Only Title Only Author and Title](#)

Gruntman E, Qi Y, Slotkin RK, Roeder T, Martienssen RA, Sachidanandam R (2008) Kismeth: analyzer of plant methylation states through bisulfite sequencing. *BMC Bioinformatics* 9: 371

Pubmed: [Author and Title](#)

CrossRef: [Author and Title](#)

Google Scholar: [Author Only Title Only Author and Title](#)

Gu X, Wang Y, He Y (2013) Photoperiodic regulation of flowering time through periodic histone deacetylation of the florigen gene FT. *PLoS Biol* 11: e1001649

Pubmed: [Author and Title](#)

CrossRef: [Author and Title](#)

Google Scholar: [Author Only Title Only Author and Title](#)

He Y (2012) Chromatin regulation of flowering. *Trends Plant Sci* 17: 556-562

Pubmed: [Author and Title](#)

CrossRef: [Author and Title](#)

Google Scholar: [Author Only Title Only Author and Title](#)

Henikoff S, Shilatifard A (2011) Histone modification: cause or cog? *Trends Genet* 27: 389-96

Pubmed: [Author and Title](#)

CrossRef: [Author and Title](#)

Google Scholar: [Author Only Title Only Author and Title](#)

Jaeger KE, Wigge PA (2007) FT protein acts as a long-range signal in *Arabidopsis*. *Curr Biol* 17: 1050-1054

Pubmed: [Author and Title](#)

CrossRef: [Author and Title](#)

Google Scholar: [Author Only Title Only Author and Title](#)

Jiang D, Wang Y, Wang Y, He Y (2008) Repression of FLOWERING LOCUS C and FLOWERING LOCUS T by the *Arabidopsis* Polycomb repressive complex 2 components. *PLoS ONE* 3: e3404

Pubmed: [Author and Title](#)

CrossRef: [Author and Title](#)

Google Scholar: [Author Only Title Only Author and Title](#)

Kozaki A, Hake S, Colasanti J (2004) The maize ID1 flowering time regulator is a zinc finger protein with novel DNA binding properties. *Nucleic Acids Res* 32: 1710-1720

Pubmed: [Author and Title](#)

CrossRef: [Author and Title](#)

Google Scholar: [Author Only Title Only Author and Title](#)

Lauria M, Rossi V (2011) Epigenetic control of gene regulation in plants. *Biochim Biophys Acta* 1809: 369-378

Pubmed: [Author and Title](#)

CrossRef: [Author and Title](#)

Google Scholar: [Author Only Title Only Author and Title](#)

Lazakis CM, Coneva V, Colasanti J (2011) ZCN8 encodes a potential orthologue of *Arabidopsis* FT that integrates both endogenous and photoperiod flowering signals in maize. *J Exp Bot* 62: 4833-4842

Pubmed: [Author and Title](#)

CrossRef: [Author and Title](#)

Google Scholar: [Author Only Title Only Author and Title](#)

Locatelli S, Piatti P, Motto M, Rossi V (2009) Chromatin and DNA modifications in Opaque2-mediated regulation of gene transcription during maize endosperm development. *Plant Cell* 21: 1410-1427

Pubmed: [Author and Title](#)

CrossRef: [Author and Title](#)

Downloaded from www.plantphysiol.org on June 6, 2017 - Published by www.plantphysiol.org
Copyright © 2015 American Society of Plant Biologists. All rights reserved.

Google Scholar: [Author Only](#) [Title Only](#) [Author and Title](#)

López-González L, Mouriz A, Narro-Diego L, Bustos R, Martínez-Zapater JM, Jarillo JA, Piñeiro M (2014) Chromatin-dependent repression of the *Arabidopsis* floral integrator genes involves plant specific PHD-containing proteins. *Plant Cell* 26: 3922-3938

Pubmed: [Author and Title](#)

CrossRef: [Author and Title](#)

Google Scholar: [Author Only](#) [Title Only](#) [Author and Title](#)

Luo C, Sidote DJ, Zhang Y, Kerstetter RA, Michael TP, Lam E (2013) Integrative analysis of chromatin states in *Arabidopsis* identified potential regulatory mechanisms for natural antisense transcript production. *Plant J* 73: 77-90

Pubmed: [Author and Title](#)

CrossRef: [Author and Title](#)

Google Scholar: [Author Only](#) [Title Only](#) [Author and Title](#)

Makarevitch I, Eichten SR, Briskine R, Waters AJ, Danilevskaya ON, Meeley RB, Myers CL, Vaughn MW, Springer NM (2013) Genomic Distribution of Maize Facultative Heterochromatin Marked by Trimethylation of H3K27. *Plant Cell* 25: 780-793

Pubmed: [Author and Title](#)

CrossRef: [Author and Title](#)

Google Scholar: [Author Only](#) [Title Only](#) [Author and Title](#)

Mascheretti I, Battaglia R, Mainieri D, Altana A, Lauria M, Rossi V (2013) The WD40-repeat proteins NFC101 and NFC102 regulate different aspects of maize development through chromatin modification. *Plant Cell* 25: 404-420

Pubmed: [Author and Title](#)

CrossRef: [Author and Title](#)

Google Scholar: [Author Only](#) [Title Only](#) [Author and Title](#)

Matsubara K, Yamanouchi U, Wang ZX, Minobe Y, Izawa T, Yano M (2008) Ehd2, a rice ortholog of the maize INDETERMINATE1 gene, promotes flowering by up-regulating Ehd1. *Plant Physiol* 148: 1425-1435

Pubmed: [Author and Title](#)

CrossRef: [Author and Title](#)

Google Scholar: [Author Only](#) [Title Only](#) [Author and Title](#)

Meng X, Muszynski MG, Danilevskaya ON (2011) The FT-like ZCN8 gene functions as a floral activator and is involved in photoperiod sensitivity in maize. *Plant Cell* 23: 942-960

Pubmed: [Author and Title](#)

CrossRef: [Author and Title](#)

Google Scholar: [Author Only](#) [Title Only](#) [Author and Title](#)

Miller TA, Muslin EH, Dorweiler JE (2008) A maize CONSTANS-like gene, conz1, exhibits distinct diurnal expression patterns in varied photoperiods. *Planta* 227: 1377-1388

Pubmed: [Author and Title](#)

CrossRef: [Author and Title](#)

Google Scholar: [Author Only](#) [Title Only](#) [Author and Title](#)

Muszynski MG, Dam T, Li B, Shirbroun DM, Hou ZL, Bruggemann E, Archibald R, Ananiev EV, Danilevskaya ON (2006) Delayed flowering1 encodes a basic leucine zipper protein that mediates floral inductive signals at the shoot apex in maize. *Plant Physiol* 142: 1523-1536

Pubmed: [Author and Title](#)

CrossRef: [Author and Title](#)

Google Scholar: [Author Only](#) [Title Only](#) [Author and Title](#)

Park SJ, Kim SL, Lee S, Je BI, Piao HL, Park SH, Kim CM, Ryu, CH, Park SH, Xuan YH, et al (2008) Rice Indeterminate 1 (OsId1) is necessary for the expression of Ehd1 (Early heading date 1) regardless of photoperiod. *Plant J* 56: 1018-1029

Pubmed: [Author and Title](#)

CrossRef: [Author and Title](#)

Google Scholar: [Author Only](#) [Title Only](#) [Author and Title](#)

Regulski M, Lu Z, Kendall J, Donoghue MT, Reinders J, Llaca V, Deschamps S, Smith A, Levy D, McCombie WR, et al (2013) The maize methylome influences mRNA splice sites and reveals widespread paramutation-like switches guided by small RNA. *Genome Res* 23: 1651-1662

Pubmed: [Author and Title](#)

CrossRef: [Author and Title](#)

Google Scholar: [Author Only](#) [Title Only](#) [Author and Title](#)

Rossi V, Locatelli S, Varotto S, Donn G, Pirona R, Henderson DA, Hartings H, Motto M (2007) Maize histone deacetylase hda101 is involved in plant development, gene transcription, and sequence-specific modulation of histone modification of genes and repeats. *Plant Cell* 19: 1145-1162

Pubmed: [Author and Title](#)

CrossRef: [Author and Title](#)

Google Scholar: [Author Only](#) [Title Only](#) [Author and Title](#)

Samach A, Onouchi H, Gold SE, Ditta GS, Schwarz-Sommer Z, Yanofsky MF, Coupland G (2000) Distinct roles of CONSTANS target genes in reproductive development of *Arabidopsis*. *Science* 288: 1613-1616

Pubmed: [Author and Title](#)

CrossRef: [Author and Title](#)

Google Scholar: [Author Only](#) [Title Only](#) [Author and Title](#)

Sekhon RS, Briskine R, Hirsch CN, Myers CL, Springer NM, Buell CR, de Leon N, Kaepller SM (2013) Maize gene atlas developed by RNA sequencing and comparative evaluation of transcriptomes based on RNA sequencing and microarrays. *PLoS ONE* 8: e61005

Pubmed: [Author and Title](#)

CrossRef: [Author and Title](#)

Google Scholar: [Author Only Title Only Author and Title](#)

Sun C, Fang J, Zhao T, Xu B, Zhang F, Liu L, Tang J, Zhang G, Deng X, Chen F, et al (2012) The histone methyltransferase SDG724 mediates H3K36me2/3 deposition at MADS50 and RFT1 and promotes flowering in rice. Plant Cell 24: 3235-3247

Pubmed: [Author and Title](#)

CrossRef: [Author and Title](#)

Google Scholar: [Author Only Title Only Author and Title](#)

Tiwari SB, Shen Y, Chang H-C, Hou Y, Harris A, Ma SF, McPartland M, Hymus GJ, Adam L, Marion C, et al. (2010) The flowering time regulator CONSTANS is recruited to the FLOWERING LOCUS T promoter via a unique cis-element. New Phytol 187: 57-66

Pubmed: [Author and Title](#)

CrossRef: [Author and Title](#)

Google Scholar: [Author Only Title Only Author and Title](#)

Turck F, Roudier F, Farrona S, Martin-Magniette ML, Guillaume E, Buisine N, Gagnot S, Martienssen RA, Coupland G, Colot V (2007) Arabidopsis TFL2/LHP1 specifically associates with genes marked by trimethylation of histone H3 lysine 27. PLoS Genet 3: e86

Pubmed: [Author and Title](#)

CrossRef: [Author and Title](#)

Google Scholar: [Author Only Title Only Author and Title](#)

Turck F, Fornara F, Coupland G (2008) Regulation and identity of florigen: FLOWERING LOCUS T moves center stage. Annual Rev Plant Biol 59: 573-594

Pubmed: [Author and Title](#)

CrossRef: [Author and Title](#)

Google Scholar: [Author Only Title Only Author and Title](#)

Wang Y, Gu X, Yuan W, Schmitz RJ, He Y (2014) Photoperiodic control of the floral transition through a distinct polycomb repressive complex. Dev Cell 28: 727-736

Pubmed: [Author and Title](#)

CrossRef: [Author and Title](#)

Google Scholar: [Author Only Title Only Author and Title](#)

Wigge PA, Kim MC, Jaeger KE, Busch W, Schmid M, Lohmann JU, Weigel D (2005) Integration of spatial and temporal information during floral induction in Arabidopsis. Science 309: 1056-1059

Pubmed: [Author and Title](#)

CrossRef: [Author and Title](#)

Google Scholar: [Author Only Title Only Author and Title](#)

Wong AY, Colasanti J (2007) Maize floral regulator protein INDETERMINATE1 is localized to developing leaves and is not altered by light or the sink/source transition. J Exp Bot 58: 403-414

Pubmed: [Author and Title](#)

CrossRef: [Author and Title](#)

Google Scholar: [Author Only Title Only Author and Title](#)

Wu CY, You CJ, Li CS, Long T, Chen GX, Byrne ME, Zhang QF (2008) RID1, encoding a Cys2/His2-type zinc finger transcription factor, acts as a master switch from vegetative to floral development in rice. Proc Nat Acad Science USA 105: 12915-12920

Pubmed: [Author and Title](#)

CrossRef: [Author and Title](#)

Google Scholar: [Author Only Title Only Author and Title](#)

Young MD, Willson TA, Wakefield MJ, Trounson E, Hilton DJ, Blewitt ME, Oshlack A, Majewski IJ (2011) ChIP-seq analysis reveals distinct H3K27me3 profiles that correlate with transcriptional activity. Nucleic Acids Res 39: 7415-7427

Pubmed: [Author and Title](#)

CrossRef: [Author and Title](#)

Google Scholar: [Author Only Title Only Author and Title](#)